Title

A genome-wide CRISPR screen highlights cationic amino acid homeostasis as a regulator of lysosomal pH

ISBN

9798293851492

Author

Welch, Mackenzie

Publication Date

2025-09-19

Peer reviewed|Thesis/dissertation

A genome-wide CRISPR screen highlights cationic amino acid homeostasis as a regulator of lysosomal pH

by
Mackenzie Welch

DISSERTATION
Submitted in partial satisfaction of the requirements for degree of
DOCTOR OF PHILOSOPHY

in

Neuroscience

in the

GRADUATE DIVISION
of the
UNIVERSITY OF CALIFORNIA, SAN FRANCISCO

Approved:

DocuSigned by:
Martin Kampmann
03BA4012CC044AF...
Martin Kampmann
Chair

DocuSigned by:
Aimee Kao
Aimee Kao

DocuSigned by:
Rushika Perera
Rushika Perera

DocuSigned by:
MICHAEL GRABE
5B8B990D587B414...
MICHAEL GRABE

Committee Members

Acknowledgements

My deepest gratitude to the following people:

I want to thank my advisor Dr. Aimee Kao, without whom this work would not have been possible. As my advisor, Aimee always brought a unique perspective and thought process to our work. Your mentorship is what made this work possible, and I have grown as a scientist from my time in your lab.

I want to thank my thesis committee Dr. Martin Kampmann, Dr. Rushika Perera, and Dr. Michael Grabe for helping guide this work over the years. The suggestions and advice you gave me made this project stronger and I thank you for it.

I also want to thank all the members of the Kao lab past and present. Graduate school is inherently challenging and stressful, but having a constant group happy to collaborate, chat or grab a coffee makes a huge difference. This process would have been much more difficult without you all.

To my friends and family, thank you for your support and listening to me over the years. I couldn't have done it without you all.

A genome-wide CRISPR screen highlights cationic amino acid homeostasis as a regulator of lysosomal pH

Mackenzie Welch

Abstract

Lysosomes are critical organelles for maintaining proteostasis in cells. One of the defining characteristics of lysosomes is their relative acidity compared to other subcellular compartments. This acidic pH is critical for the efficient breakdown of macromolecules and cellular homeostasis, and disruptions in lysosomal pH homeostasis have been linked to aging and disease. The mechanisms through which lysosomal pH is maintained are incompletely understood, a question important in neurons which are susceptible to age associated decline in proteostasis. Supporting this, we found neuronal lysosomes have a unique pH optimum for tau degradation. To better understand neuronal lysosomal pH regulation, we conducted a genome-wide CRISPRi-based screen in iPSC derived neurons for modifiers of lysosomal pH. We validated several previously known regulators of lysosomal pH and discovered novel pathways capable of modifying lysosomal pH including the protein UFMylation and mitochondrial integrity. We demonstrate that loss of lysosomal cationic amino acid exporter, PQLC2, strongly increases lysosomal pH, and we link this increase in lysosomal pH to an accumulation of amino acids within the lysosome. Our results highlight novel genes underpinning lysosomal pH homeostasis and represent potential novel targets for neurodegenerative disease treatment.

Table of Contents

List of Figures

List of Abbreviations

BDNF	Bone derived neurotrophic factor
BafA1	Bafilomycin A-1
BDNF	Bone derived neurotrophic factor
CTSB	Cathepsin B
CRISPRi	CRISPR interference
DMSO	Dimethyl sulfoxide
FDR	False discovery rate
FIREpHLy	Fluorescence indicator reporting pH in ysosomes
FACS	Fluorescence-activated cell sorting
GO	Gene ontology
IP	Immunoprecipitation
iPSC	Induced pluripotent stem cell
iNeuron	Induced pluripotent stem cell derived neuron
mTOR	Mamalian target of rapamycin
mTFP1	Monomeric teal fluorescent protein
MOI	Multiplicity of infection
NGN2	Neurogenin-2
NT-3	Neurotrophin-3
NTC	Non-targeting control
V-ATPase	Vacuolar H+-ATPase

Chapter 1: Lysosomal pH homeostasis and its role in disease

1.1 Lysosomal pH regulation

Cellular proteostasis is reliant on the effective degradation of protein to maintain cell health. The lysosome and proteosome act in tandem to maintain the balance of protein translation and degradation, but these pathways can become dysregulated with aging or disease [1]. The lysosome is the primary pathway for clearance of large protein aggregates and organelles [2, 3], and its proper functioning is critical for cell health. The degradative capacity of the lysosome is enabled by its resident hydrolases which are responsible for the digestion of protein, lipids and carbohydrates. A greater understanding of how the cell regulates lysosomal clearance of substrates might reveal novel autophagy modulating therapeutics.

The lysosome is defined in part by its low pH relative to the rest of the cell. Compared to other organelles, the lysosomal lumen is the most acidic location within the cell with a pH of ~4.5-5. The low pH of the lysosome is maintained by the proton import activity of the vacuolar H+ ATPase (V-ATPase) which is offset by a number of counter-ion channels to decrease lysosomal membrane potential [4–7]. Many of the channels that contribute to lysosomal pH homeostasis have links to lysosomal storage disorders or neurodegenerative disease [8, 9].

As the import pathway for protons, the V-ATPase plays an integral role in maintaining homeostatic lysosomal pH. The regulation of the complex's activity is in part how homeostatic lysosomal pH is maintained. However as the V-ATPase is localized to many organelles including

but not limited to synaptic vesicles, endosomes, and the golgi complex [10], the low pH of the lysosome cannot be simply explained by the activity of the V-ATPase as the different compartments have unique pH requirements. The activity of the V-ATPase is in part regulated by its assembly, as the V_1 and V_0 subdomains of the complex can be reversibly assembled to increase or decrease its activity [10]. A number of factors have been identified to regulate this process, including the proteins Regulator of H+-ATPase of vacuoles and endosomes (RAVE), the PKA pathway, and the lipid $PI(3,5)P_2$ [11–13]. Importantly, this assembly is also regulated both by nutrient availability and mTOR activity [14, 15], and is one mechanism the cell uses to modulate lysosomal pH and lysosome activity. Activity of mTORC can also be regulated by the V-ATPase in response to lysosomal amino acid availability [16] and supports the amino acids as a key mechanism of lysosomal homeostasis. This assembly is not entirely driven by nutrient availability, as V-ATPase assembly can be maintained in nutrient poor conditions by lysosomal alkalinizing agents such as chloroquine [17] indicating there are other mechanisms promoting V-ATPase assembly in response to lysosome alkalinization.

Lysosomes require a counter-ion pathway to reduce lysosomal membrane potential. One proposed mechanism underlying the dissipation of membrane potential is the chloride/proton antiporter, CLC-7, which has been shown to play a role in maintaining lysosomal pH [4]. CLC-7 exchanges two Cl^- and an H^+, and can promote lysosomal acidification through dissipation of positive charge in the lysosome lumen [5]. This proposed anion current is not the only proposed mechanism through which the lysosome can reduce luminal positive charge. TRPML1, and TPC1/2 have been proposed to export Ca^{2+}, Na^+ from the lysosome respectively [7, 18, 19]. These channels have been shown to play a role in lysosomal pH regulation and may work in tandem with CLC7 to maintain homeostatic lysosomal pH.

For proton leak currents, two mechanisms have been proposed: TMEM175 and SLC7A11 [6, 20]. TMEM175 was originally thought to be a lysosomal K^+ channel, but has been demonstrated to act as a H^+ leak channel at pH values below 4.5 and acts to prevent lysosomal hyper-acidification [6, 21]. As TMEM175 conductance is low at high pH, a second proton current was sought to mediate lysosomal deacidification upon v-ATPase inhibition. The identity of this unconventional proton current is the neutral amino acid exporter, SLC7A11. This transporter exports neutral amino acids from the lysosome, and behaves as an unconventional H^+ leak current at pH values above 4.5 [20] through coupling proton to amino acid export. Together these two proteins represent the proton leak current involved in maintaining lysosomal pH homeostasis.

1.2 Neurodegenerative disease and lysosomal pH dysfunction

Neurodegenerative diseases are a group of disorders that are characterized by the progressive loss of neurons and neuronal function. These disorders represent a growing patient population as the average age of the country rises [22]. To date, there are few effective treatments for these disorders, with many of the current therapies addressing disease symptoms as opposed to being disease modifying therapies. To effectively develop drugs to treat these indications, there is still a gap in our understanding about the biological mechanisms underlying these diseases' development and progression.

Many of the genes that confer neurodegenerative disease risk converge on the endolysosomal pathway [23, 24]. This highlights the particular importance of autophagy and the lysosome for the clearance of neurodegenerative disease substrates, and mutations in disease proteins can alter substrate clearance by lysosomal proteases [25]. When cells cannot clear

proteins, they become sequestered in the form of aggregates which are one of the defining characteristics of neurodegenerative disease [26].

Disruptions in lysosomal pH are a phenotype observed in a number of neurodegenerative disease models [27–31]. Loss of either of the two lysosomal proteins that support the H^+ leak current, TMEM175 and SLC7A11, result in both decreased lysosomal pH and alpha synuclein accumulation. This accumulation of alpha synuclein can be reversed with low doses of lysosome alkalinizing drugs in vitro [6, 20]. Over-expression of wild-type alpha synuclein has also been linked to increased lysosomal pH in vitro, and its accumulation can be ameliorated through re-acidification of lysosomes [32]. This nicely demonstrates the specific pH optima of the lysosome for substrate clearance, as deviations in either the acidic or basic direction result in accumulation of alpha synuclein.

One common mechanism shared by several neurodegenerative disease genes is regulating the activity of the V-ATPase. Both PSEN1 and APP mutants modify the assembly and activity of the V-ATPase in models of Alzheimer's disease [27, 33]. Both LRRK2 and TMEM106B have been found to directly interact with the v-ATPase to modify lysosomal pH, and result in lysosomal pH dysfunction when this interaction is lost [30, 34]. The convergence of V-ATPase dysregulation across multiple neurodegenerative diseases demonstrates lysosomal pH's central role in disease pathogenesis. For the purposes of understanding and treating neurodegenerative disease, improving our understanding of how lysosomal pH is regulated is an important strategy for untangling what is a shared mechanism across different diseases.

2.3 Aging and lysosomal pH dysregulation

Importantly, one of the primary risk factors for the development of neurodegenerative disease is increased age. The average age of onset is over 55 years old for Alzheimer's, Parkinsons or Frontotemporal Dementia and incidence of these disorders rises with increasing age [35]. It is important to look for processes that are dysregulated in both neurodegenerative disease and aging as we strive to understand what underlies the strong association between age and neurodegeneration.

Autophagy decline is a hallmark of the aging process [36]. As part of that decline, it was first demonstrated that the yeast vacuole progressively alkalinizes with increased replicative age [37]. Since then, this association between age and lysosomal pH has been shown in *Caenorhabditis elegans* (C. Elegans) intestinal cells [38]. Both studies find that lifespan and lysosomal pH linked and demonstrate that manipulations altering either lifespan or lysosomal pH can affect the other. In yeast, overexpression of v-ATPase subunits increases the replicative age possible before death, and in *C. Elegans* long-lived *daf2* mutants maintain acidic lysosomal pH for longer [37, 38]. Taken together, lysosomal pH links both aging and neurodegenerative disease as a common hallmark of both processes.

Chapter 2: A genome-wide CRISPR screen highlights cationic amino acid homeostasis as a regulator of lysosomal pH

2.1 Introduction

Lysosomes are acidic, membrane-bound organelles serving as one of the primary methods of protein degradation within the cell [1]. In addition to protein degradation, the lysosome plays a central role in processes including regulating autophagy [39], nutrient sensing [16], and calcium signaling [7]. Likely because small changes in pH can have dramatic effects on protein structure [40], optimal lysosomal function relies heavily on maintenance of an acidic environment within the lysosome, with resident proteins having a pH optimum tuned to ~4.5-5.0 [41]. Lysosomal acidic pH is achieved through multiple concurrent processes: the import of protons by the vacuolar-type H^+-ATPase (V-ATPase) [10], which is offset by counter-ion currents from other lysosomal channels which act to prevent an increase in lysosomal membrane potential [5]. Without proper lysosomal acidification through the action of these channels and transporters, resident lysosomal proteins function both sub-optimally and can drive changes in protease substrate specificity [25, 42].

Given the importance of lysosomal acidification, it is not surprising that disruptions in lysosomal pH have been found in aging and neurodegeneration [37, 38]. In models of aging, the acidic organelle displays a progressive alkalinization. Genetic models of neurodegenerative diseases have also demonstrated impairments in lysosomal pH homeostasis [27, 30, 31, 43].

Notably, recent work has shown lysosomal pH alkalinization precedes cell death and amyloid beta deposition in a mouse model of Alzheimer's disease [28]. Restoration of lysosomal pH homeostasis can reduce the accumulation of alpha-synuclein in cell models of Parkinson's disease [32]. Importantly, a primary risk factor for neurodegenerative disease is increased age [44], thus lysosomal pH dysregulation may represent a potential link between aging and neurodegeneration.

Systematic efforts to understand how neuronal lysosomal pH is maintained are lacking. This has been in part due to a lack of appropriate tools for large-scale experiments involving lysosomal pH. Previous methods for measuring lysosomal pH have relied on pH-sensitive fluorescent molecules such as Lysosensor or Oregon Green 488, either as free dyes or dextran-conjugates [45]. These methods present a challenge for large-scale studies like genetic screens due to challenges in delivery, cost, and potential for lysosomal pH disruption [29]. To overcome these limitations, our group recently developed a genetically encoded lysosomal pH sensor, Fluorescence Indicator REporting pH in Lysosomes (FIRE-pHLy) [46]. We have shown that FIRE-pHLy is amenable to high-throughput applications through a prior screen to identify novel compounds capable of acidifying lysosomes [47].

Given the importance of lysosomal pH in aging and neurodegeneration, we undertook a genome-wide CRISPRi screen for modifiers of lysosomal pH in human induced pluripotent stem cell (iPSC)-derived neurons (iNeurons). In addition to confirming previously reported modifiers of lysosomal pH, our screen identified several lysosomal substrate exporters and genes involved with amino acid regulation of mTORC1 as potent, previously unidentified modifiers of neuronal lysosomal pH. Numerous pathways previously unlinked to lysosomal pH including protein UFMylation and mitochondrial health were represented within our screen. Of these hits, the

cationic amino acid exporter PQLC2 was one of our strongest lysosome-localized hits and represents a previously unidentified lysosome protein involved in maintenance of lysosomal pH. We demonstrated PQLC2 also operates as an important contributor for maintenance of lysosomal pH through the export of basic amino acids from the lysosomal lumen. Together, this study reveals novel genes that modify lysosomal pH and highlight possible new targets for ameliorating age-related lysosome dysfunction.

2.2 Results

2.2.1 Lysosomes isolated from human iPSCs and neurons differ in optimal pH for Tau cleavage but not BSA or TDP-43

An acidic lysosomal pH is known to be important for lysosomal protease activity, but the extent that small deviations from a pH optimum can alter degradation of a disease associated neuronal substrates are unknown. Our group has previously demonstrated neurodegenerative disease-associated proteins such as TDP-43 and tau have specific pH optima for a given individual lysosomal hydrolase [25]. We tested the proteolysis capacity of isolated lysosomes at stepwise pH set points. We first transduced our iPSCs with the LysoIP tag, a 3X HA-tagged TMEM192 localized to lysosomes, and isolated lysosomes from both iPSCs and induced neurons through immunoprecipitation [48]. Isolated lysosomes from iPSCs or iNeurons were then incubated with recombinant TDP-43 or tau. Surprisingly, we found iPSC-derived lysosomes degraded tau at higher pH, with complete cleavage occurring by 30 minutes at pH 5.0 (**Figure 2.5.1 A, B**) compared to pH 3.5, which only had partial cleavage. Conversely, neuronal lysosomes had minimal cleavage of tau at pH 5.0 but had a unique optimum at pH 4.0 (**Figure 2.5.1 C, D**) with

the highest amount of protein digestion. These results indicate that neuronal lysosomes may have distinct pH requirements for substrate degradation compared to other cell types. In contrast to tau, TDP-43 did not demonstrate a unique pH optimum for digestion by neuronal lysosomes (**Figure 2.5.1 E-F**). These findings support a role for lysosomal pH in digestion of certain neurodegenerative disease associated proteins such as tau.

We next tested cleavage of a generic substrate to see if neuronal lysosomes had a unique optimum for peak digestion, or if this effect was limited to tau. For our generic control, we measured the rate of cleavage of the cleavage reporter, DQ-BSA. DQ-BSA is a quenched Bodipy labelled BSA that fluoresces when cleaved. We observed no differences in BSA degradation after incubation with either iPSC-derived or neuronal lysosomes (**Figure 2.5.2 A-D**). From these data, it appears neuronal lysosomes are finely tuned to degrade certain substrates associated with neurodegenerative disease compared to iPSC lysosomes. To date, regulation of how lysosomal pH is regulated is incompletely understood which prompted us to embark on a screening effort to understand how neuronal lysosomal pH was regulated.

2.2.2 Genome-wide screen for neuronal lysosomal pH modifiers

We utilized a novel, genetically encoded lysosomal pH sensor, FIRE-pHLy, in a CRISPRi screen for modifiers of lysosomal pH in human iNeurons. FIRE-pHLy consists of a luminal-facing pH-sensitive fluorophore, mTFP, fused to lysosomal-associated membrane protein 1 (LAMP1) for lysosome targeting and a cytosol-facing mCherry for ratiometric measurement (**Figure 2.5.3 A**) [46]. We transduced doxycycline-inducible neurogenin 2 (NGN2) iPSCs with lentivirus expressing the FIRE-pHLy construct and validated that the sensor was working appropriately in iPSC-derived neurons by treating them with bafilomycin overnight.

The ratio of mTFP/mCherry increased with bafilomycin, indicating elevated lysosomal pH compared to the DMSO control (**Figure 2.5.3 B)**. To ensure our reporter was properly trafficked to lysosomes in iPSC-derived neurons, we measured colocalization between our sensor and the lysosome marker LAMP2. We found FIRE-pHLy colocalized with LAMP2 (R=0.9) compared to mitochondria (R=0.5, $p<0.05$) (**Figure 2.5.3 C,D**).

Once we were confident that FIRE-pHLy performed appropriately in neurons, we undertook a whole-genome screen for lysosomal pH modifiers in iPSC-derived Neurons. We transduced FIRE-pHLy into induced pluripotent stem cells (iPSCs) containing both CRISPR interference (CRISPRi) and doxycycline inducible NGN2 neuronal differentiation machinery [49]. To perform the screen, iPSCs were transduced with lentivirus targeting all coding genes [50], selected for 5 days with puromycin, and differentiated into neurons. On day 14, the neurons were dissociated, FACS-sorted based on ratio of mTFP signal to mCherry signal, and the top and bottom 30% were collected (**Figure 2.5.4**). After sample processing, sgRNA frequencies within each fraction were quantified via next-generation sequencing and compared to non-targeting controls (NTC) using a Mann-Whiteney U test to assign p-values for each gene. Based on a false discovery rate (FDR) of 5%, 1,050 genes were called hits. Roughly 3/4 of the hits resulted in an alkaline lysosomal pH phenotype with the remaining 1/4 resulting in an acidic phenotype. For clarity, genes with an alkaline phenotype will be referred to as alkalinizing hits and genes that have an acidic phenotype will be referred to as acidic hits.

For our alkalinizing hits, the screen identified both established and novel pathways. Reassuringly, Gene Ontology (GO) enrichment analysis identified vacuolar acidification and positive regulation of mTOR signaling in lysosomal pH regulation as alkalinizing hits (**Figure 2.5.3 G)** [15, 47]. Individual proteins within this set of lysosomal pH modifiers included *CLCN7*,

OSTM1, TMEM106B, MCOLN1, PIKFYVE and multiple v-ATPase subunits, all of which are previously reported to contribute to lysosomal pH acidification [4, 34, 51, 52]. These hits support the biological relevance of our dataset and suggest that the group of genes that are found among the alkalinizing hits normally functions to promote lysosomal acidification.

GO enrichment analysis of alkalinizing hits also highlighted novel pathways contributing to lysosomal pH acidification: mitochondrial translation and mitochondrial complex I assembly as the two most enriched categories (**Figure 2.5.3 G**). Acidifying the lysosome is an energetically costly process, requiring V-ATPase transport of protons into the lysosomal lumen through hydrolysis of ATP [10]. This highlights the importance of mitochondria and ATP generation on lysosome homeostasis.

Among the acidifying hits, several GO categories of interest were identified. Every member of the UFM1 conjugation pathway (*UFM1*, *UFL1*, *UBA5*, *DDRGK1*, *CDK5RAP3* and *UFC1*) was enriched within the acidifying hits portion of our screen (**Figure 2.5.3 H**). Protein UFMylation is a ubiquitin-like process recently identified to be a modifier of tau homeostasis [54, 55]. Previous work has linked deficiency of DDRGK1 to autophagy induction with dysfunctional lysosomes [56], indicating our acidic phenotype might be due to accumulation of hyper-acidic, dysfunctional lysosomes.

We next examined for lysosomal pH modifiers in our dataset more proximal to the lysosome and autophagy. Our GO enrichment analysis highlighted both regulation of mTORC and autophagy (**Figure 2.5.3 G,H**). The categories included components of the Ragulator/RAG complex and amino acid sensing machinery regulating mTORC. It has been established that both mTORC1 inhibition and amino acid starvation are capable of modulating lysosomal pH [15, 47,

57]. Notably, one of our strongest alkaline hits, PQLC2, recently was found to signal cationic amino acid availability to mTORC1 [58, 59].

2.2.3 Lysosomal pH modifier screen validation through sub-library screening

To validate the whole-genome screen results, we constructed a lysosomal pH sub-library consisting of 212 control sgRNAs and 831 of the highest-scoring hits from the whole genome screen, hits annotated as lysosomal resident proteins, and hits annotated as linked to neurodegenerative disease. This sub-library was then deployed in two parallel approaches. First, we repeated the FACS-based FIRE-pHLy iNeuron screen (**Figure 2.5.5 A**). Results from this FIRE-pHLy sub-library screen exhibited high correlation with the initial whole genome screen (**Figure 2.5.5 B**), highlighting the reproducibility of the initial screen hits when tested with a smaller sgRNA library at a higher coverage.

Next, we tested the sub-library using an orthogonal measure of lysosomal pH, Oregon Green dextran. as the pH sensitive dye and CF555 as the pH insensitive endocytosis control. This orthogonal screen could also serve to potentially identify hits that modify expression or trafficking of the FIRE-pHLy sensor. Induced neurons were incubated with the two labelled dextrans overnight, washed with neuronal media and followed by a 4-hour incubation in fresh media to allow time for the dextrans to traffic to the lysosome. The cells were then dissociated and FACS sorted based on their Oregon green to CF555 ratio.

In comparing our FIRE-pHLy and dextran-based pH sublibrary screens, we noted the two pH methods had limited correlation with one another (**Figure 2.5.5 C**). This was driven in part by several genes with opposing phenotypes based on the measurement method. Of these genes, a number of them regulate either endosomal transport or cellular protein trafficking including

WDR91, *GNPTAB*, *RAB3GAP1* and *RAB1A* [60–62] which may be the result of potential differences in trafficking of either sensor. While the correlation between the two screens was low, several genes validated appropriately in both datasets including PQLC2, components of the UFM1 pathway, and mitochondrial genes with a greater degree of overlap coming from genes resulting in an alkaline lysosomal pH phenotype (**Figure 2.5.5 C-E**). Together, these two approaches underscore both the methodological differences between genetically encoded and endocytic pH sensors, and the robustness of hits identified by both.

In parallel, we validated our pooled FACS screening results by a microscopy-based method utilizing individually cloned sgRNA cell lines. We selected a subset of genes of interest from our whole genome screen and generated individual sgRNA iPSC lines. Briefly, iPSCs expressing FIRE-pHLy were transfected with high scoring guides from the whole genome screen alongside two non-targeting controls, differentiated and plated into 96 well imaging plates. On day 14, the cells were fixed in 2% PFA and imaged with an IN Cell Analyzer 6500 as previously described [47]. Positive or negative hits were called based on changes greater than 3-fold the standard deviation of the non-targeting controls. Of the nine tested alkalinizing hits, eight showed the same phenotype in cell lines, whereas only 5 out of the 10 tested acidifying hits showed a decrease in lysosomal pH (**Figure 2.5.5 F**). Similarly to the sub-library validation screens, we found our alkaline hits validate more consistently compared to our acidic hits when using an imaging-based methodology. Based on both of our validation efforts, we concluded our sensor had a greater dynamic range towards lysosomal alkalinization and focused primarily on our alkaline hits for further characterization.

2.2.4 PQLC2 expression modulates lysosomal pH in multiple cell types

PQLC2 emerged as one of our strongest lysosome-localized hits (**Figure 2.5.3E**). PQLC2 is cationic amino acid transporter in the lysosomal amino acid exporter family of solute carrier membrane proteins. It is a lysosomal resident protein that mediates the efflux of basic amino acids (arginine, lysine and histidine) from the lysosomal lumen [63], and loss of PQLC2 results in the accumulation of these amino acids in the lysosome [64] indicating it is the primary export pathway. PQLC2 also recruits the C9Orf72-SMCR8-WDR41 complex to the lysosomal surface [58]. Given its role in lysosomal function, we sought to further characterize the role of PQLC2 in lysosomal pH regulation and protein homeostasis more broadly. We generated both a PQLC2 CRISPRi knockdown cell line in the WTC11 iPSC background [65], as well as a PQLC2 CRISPR knockout cell line in the KOLF2.1J background [66], ensuring robustness of our findings across genotypes. For the CRISPR knockout lines, we evaluated two clones and confirmed knockout by Sanger sequencing paired with ICE analysis (**Figure 2.5.7A, B**). PQLC2 knockdown by CRISPRi confirmed by qPCR with a greater than 95% decrease in *PQLC2* mRNA levels (**Figure 2.5.7 C**).

To investigate the role of PQLC2 on lysosomal pH, we transduced both our CRISPRi and CRISPRko cell lines with FIRE-pHLy. After neuronal differentiation, both neuronal lines showed increased mTFP to mCherry ratio indicative of increased lysosomal pH (**Figure 2.5.6A, B**). We further validated this phenotype through use of our orthogonal dextran-based approach. Neurons were incubated overnight with both Oregon Green-488 dextran and CF555 dextran and washed with fresh media the following morning. After a 4-hour chase period for the dextrans to fully reach the lysosomal compartments, we measured the ratio between the two dyes. Consistent with our FIRE-pHLy findings, we observed PQLC2-deficient neurons had increased lysosomal

pH based on their Oregon Green to CF555 ratio (**Figure 2.5.6B, F**). Together, these results demonstrate that loss of PQLC2 elevates lysosomal pH across multiple genetic backgrounds, supporting a direct role for PQLC2 in maintaining lysosomal pH homeostasis.

To determine the absolute change in lysosomal pH upon loss of PQLC2, we used PQLC2 knockout HEK293FT cells [58] and measured lysosomal pH using Oregon Green-488 dextran and a set of pH calibration buffers adapted from a previously published protocol [67]. In brief, cells were loaded with Oregon Green-488 dextran overnight and washed with fresh media five times the following morning. The dextrans were chased to the lysosome for four hours prior to imaging. The pH-sensitive wavelength was excited at 490 nm and the pH-insensitive wavelength was excited at 440 nm, and pH calibration was done by incubation with a series of buffers ranging from pH 3.6 to 7.0 with 10 μg/mL of both valinomycin and nigericin. We observed an increase in lysosomal pH from 4.6 to 4.9 in *PQLC2* knockout HEK293FT cells (**Figure 2.5.6C**).

To confirm the specificity of our lysosomal pH phenotype, we tested whether re-expression of PQLC2 restored normal lysosomal pH. Prior results indicated *PQLC2* is weakly expressed in iNeurons [49], so we stably expressed PQLC2 under the weak promoter PGK. When we re-expressed PQLC2 in either our PQLC2 CRISPRi or knockout lines, we saw rescue of lysosomal pH to the level of our non-targeting control (**Figure 2.5.6F, H**). These results confirm the specificity of our lysosomal pH phenotype and demonstrate that it is mediated through PQLC2 expression.

2.2.5 Loss of PQLC2 alters lysosome function

We next asked if loss of PQLC2 expression modified lysosome morphology and function. It's been previously shown increased lysosome size is linked to changes in lysosomal pH and is a characteristic of lysosomal storage diseases [68, 69]. We first measured lysosome size, and CRISPRi knockdown of PQLC2 resulted in increased lysosome size (**Figure 2.5.8A, B).** This increase in lysosome size was rescued by re-expression of PQLC2. The increased lysosomal size suggests a broader disruption of lysosomal homeostasis linked to the observed increase in lysosomal pH.

We next asked if this change in lysosomal pH modified the activity of lysosomal enzymes and their ability to degrade cargo. We first measured the activity of cathepsin B (CTSB) as it has a pH optimum higher than typical lysosomal pH [70]. In our PQLC2 knockout cells, we observed increased CTSB activity (**Figure 2.5.8C, D**) as measured by Magic Red signal. This indicates that the measured change in pH we identified is having a functional difference on lysosomal enzyme activity as the average lysosomal pH shifts towards CTSB's pH optima.

We next asked if the increase in CTSB activity would increase overall lysosomal proteolysis. We assessed this with the fluorogenic probe, DQ-BSA [71]. Neurons were incubated with DQ-BSA for four hours prior to imaging. We observed a decrease in DQ-BSA fluorescence in PQLC2 knockout cells compared to wild-type, indicative of a compromised ability of the cells to degrade BSA (**Figure 2.5.8E, F**). The loss of PQLC2 and resulting increase in lysosomal pH was sufficient to reduce BSA degradation, despite increases in CTSB activity.

2.2.6 Conserved PQ-loop motif and CSW binding are not required for maintaining lysosomal pH

To understand the mechanism behind PQLC2 loss and lysosomal alkalinization, we tested a series of mutants predicted to have a functional effect on PQLC2 function based on conservation and predicted deleterious mutants. First, we asked whether either of the two PQ-loop motifs, a conserved hallmark of PQ-loop proteins (**Figure 2.5.9A**), were involved in maintaining lysosomal pH. Prior work in *C. elegans*, have demonstrated a role of the PQ loop proteins in amino acid export [63], but this has not been established in mammalian systems. We generated PQ-loop mutants, PQLC2^{P55A}, PQLC2^{P201A} and PQLC2$^{P55A/P201A}$, and tested their ability to rescue neuronal lysosomal pH in PQLC2 knock-out cells. Surprisingly, the PQLC2^{P55A}, PQLC2^{P201A} and PQLC2$^{P55A/P201A}$ mutants all effectively restored normal lysosomal pH (**Figure 2.5.9B**), demonstrating that the two PQ-loop motifs were not involved in acidifying lysosomal pH.

We then expressed additional mutants, PQLC2^{F49A} and PQLC2^{W78A}, that have previously been shown to either fully or partially prevent binding of the CSW complex to PQLC2 [59]. Both mutants rescued to the same degree as wild-type PQLC2 (**Figure 2.5.9C**), indicating lysosomal pH is not regulated by interactions between CSW and PQLC2.

2.2.7 Charged residues within the transmembrane region of PQLC2 are required for lysosomal pH regulation

Next, we mutated the conserved R199 based on a previous report linking a homozygous PQLC2^{R199Q} mutation to autosomal recessive retinitis pigmentosa, a progressive neurodegenerative disease [72]. To test this, we mutated generated a PQLC2^{R199A} mutation, and

when PQLC2^{R199A} was expressed in PQLC2 knockout cells, it incompletely rescued lysosomal pH (**Figure 2.5.9D**), indicating that R199 is involved in PQLC2 regulation of lysosomal pH.

As arginine is a charged amino acid, we next asked if mutating the other conserved charged amino acids with the transmembrane domain, three aspartic acids at positions 82, 109 and 266, would have similar effects on lysosomal pH. After expressing either PQLC2^{D82A}, PQLC2^{D109A}, or PQLC2^{D266A} in our PQLC2 knockout cell line, we observed either no lysosomal pH rescue (PQLC2^{D109A}), or incomplete pH rescue with PQLC2^{D82A} and PQLC2^{D266A} (**Figure 2.5.9E**). Together, we demonstrated these four charged residues are involved in PQLC2 maintenance of lysosomal pH.

2.3 Discussion

Due to the association between proteostasis decline, lysosomal pH increases and protein accumulation seen in aging and neurodegeneration [1, 37, 38], understanding both how lysosomal pH is regulated and how changes in pH affect substrate degradation is important to our understanding of neurodegenerative disease pathogenesis. The effects of individual genes related to neurodegenerative disease and aging on lysosomal pH have been studied in detail, but a comprehensive, unbiased approach towards understanding lysosomal pH had not been completed. One previous studying using Lysosensor Yellow/Blue identified a small number of possible pH modifiers, however due to their methodology, the screen primarily identified genes driving formation of hyper-acidic vacuoles in HAP1 cells[73]. We utilized a genetically encoded sensor to avoid the potential pitfalls of dye-based approaches to lysosomal pH measurement. As part of our validation, we counter-screened our lysosomal pH hits with dextran-conjugated dyes, and our belief is the limited agreement between our FIRE-pHLy screens and dextran screen for

our acidifying hits represents this potential downside of pH sensitive dyes. Of the genes identified with this approach, only *PIKFYVE* was a hit within out dataset. In contrast, PIKFYVE inhibition and knockout of its accessory proteins has been linked to hyper-acidic vacuoles using either Lysosensor or dextran based approaches [4, 73] whereas FIRE-pHLy reported a strong increase in lysosomal pH in both our whole genome screen, as well as our imaging validation representing another possible difference between genetically encoded versus endocytosed sensors. We hypothesize this difference is due in part to differences in lysosomal compartments labelled by endocytosis versus LAMP1 trafficking [74]. While a genetically encoded sensor can and does have similar pitfalls, use of the two techniques in tandem is a robust strategy for finding robust modulators of lysosomal pH. Our results represent a large, robust dataset of potential targets to modulate lysosomal pH.

Prior work has demonstrated that PQLC2 knockout cells accumulate amino acids indicating it exists as the primary cationic amino acid export pathway at the lysosome [64]. We show that loss of PQLC2 results in a strong lysosomal pH phenotype, and believe this plays a role in disease pathogenesis [72, 75]. Additional work has shown that amino acid export is not proton couple, and lysine and arginine are exported as charged molecules without a bound proton [76]. We hypothesize based on our series of PQLC2 point mutants that fail to rescue lysosomal pH, that the accumulation of charged amino acids acts as a buffer increasing the pH of the lysosome. This is contrary to prior work which proposed an interaction between PQLC2 and the V-ATPase through an unknown mechanism based on their ability to co-immunoprecipitate [77]. While possible, the location of the charged residues we identified as driving a lysosomal pH phenotype, makes their role in an interaction with the V-ATPase unlikely.

Our work highlights the diversity of proteins which affect neuronal lysosomal pH and emphasizes the role of amino acid homeostasis on lysosomal pH regulation. Further work is needed to dissect how many of these identified lysosomal pH modifiers work in concert to form a lysosomal pH regulatory network.

Although our work was designed to be comprehensive, there are limitations to our study. By performing our screen in neurons, there was a potential for strong pH modifiers to drop out of our screen by the day of analysis. Prior work has shown that predicted lysosomal pH modifiers including V-ATPase components have a survival phenotype unique to neuronal survival screens [78], and could lead to an underestimation of a particular gene's lysosomal pH phenotype. Additionally, there are potential pitfalls associated with using a genetically encoded sensor such as FIRE-pHLy. As our primary screen was performed with FIRE-pHLy, genes that regulate LAMP1 trafficking or affect FIRE-pHLy degradation have the potential of changing FIRE-pHLy ratio without a corresponding change in lysosomal pH. We attempted to address this with our secondary dextran-based counter screen but both methods have the potential to misidentify or miss genuine lysosomal pH modifiers, and genes that were hits in one or the other should not be discarded without further investigation. Further work will be needed to disentangle the differences in lysosomal pH measurement observed between the two methodologies.

2.4 Methods

Protease activity assays

Protease activity assays were performed in triplicate either in black, flat-bottom 384-well plates (Corning, 3544) using 20μM DQ-BSA fluorescent substrates (ThermoFisher, D12051) with isolated lysosomes from either iPSCs or iNeurons in Eppendorf Protein LoBind Tubes (Fisher

Scientific, E925000090) using. Assays were conducted at 37 °C for up to 2 hours. The following buffers, each supplemented with 2 mM DTT and 1 mM EDTA, were used: 100 mM sodium citrate (pH 3.5, 3.75), 50 mM sodium acetate (pH 4.0, 4.25, 4.5, 4.75, 5.0). Fluorescence was monitored with a BMG Labtech VANTAstar plate reader using excitation and emission wavelengths of 485 nm and 530 nm respectively. Initial velocity (RFU/min) calculations were made using BMG Labtech's MARS Data Analysis Software

Western blots

For Western blot analysis, samples were denatured as described above and separated on pre-cast 4–12% NOVEX NuPAGE Bis-Tris gels using MOPS running buffer (Fisher Scientific, NP0001) and Invitrogen Novex Sharp Pre-Stained Protein Standards (Fisher Scientific, LC5800). Membranes were blocked at room temperature with Odyssey Blocking Buffer (LI-COR, 927-40,100) and incubated at 4 °C overnight with primary antibodies and 1 hour at room temperature with fluorescent secondary antibodies (LI-COR, 1:5000). Immunoreactive bands were visualized using a LI-COR Odyssey CLx image scanner and quantified with Image Studio version 5.5. Blots were quantified using ImageJ and GraphPad Prism (GraphPad Software, La Jolla, California USA).

Human iPSC Culture

Human iPSCs (WTC11 and KOLFj2.1 backgrounds) were cultured in Stemflex medium (ThermoFisher Scientific, A3349401) on Matrigel (Corning, 354277) coated dishes. During passaging, cells were lifted using Relesr (Stemcell Technologies, 100-0483) and then replated in media supplemented with a 10 μM ROCK inhibitor (StemCell Technologies, 72304). Studies with human iPSCs at UCSF were approved by the The Human Gamete, Embryo and Stem Cell

Research (GESCR) Committee. Informed consent was obtained from the human subjects when the WTC11 or KOLF2.1J lines were originally derived [47].

Human iPSC-derived neuron culture

iPSCs differentiation and neuronal were performed as previously described [79]. Briefly, iPSCs were plated onto Matrigel coated plates using N2-predifferentiation media. Briefly, cells were plated in Knockout DMEM (Thermo Fisher Scientific, 10-829-018) containing 2 µg/ml doxycycline, 1 µg/ml Rock inhibitor, 1X N2 (Thermo Fisher Scientific, 17502048), 1X NEAA (Thermo Fisher Scientific, 11140050), 1 µg/ml NT-3 (Thermo Fisher Scientific, #450-03), 1 µg/ml BDNF (Thermo Fisher Scientific, #450-02) and 1 µg/ml laminin (Thermo Fisher Scientific, #23-017-015). The following day, media was exchanged for fresh media without rock inhibitor. After 72 hours of NGN2 induction by doxycycline, the neurons were replated using accutase to plates precoated with PEI/laminin coated plates or chamber slides (Ibidi, 80806). PEI plates were prepared by diluting 50% PEI to 0.2% in 1x Borate buffer, added to cell culture plates and incubated at 37°C overnight. Plates were washed five times with water and allowed to dry completely prior to coating with 10 ug/ml laminin diluted in water.

After replating, neurons were maintained in N2/B27 media consisting of equal parts DMEM/F12 and Neurobasal-A, 1X NEAA, 0.5X GlutaMAX (Thermo Fisher Scientific, 35050061), 0.5X N2 Supplement, 0.5X B27 supplement (Thermo Fisher Scientific, 17504044), 1 µg/ml NT3 (Thermo Fisher Scientific, 450-03), 1 µg/ml BDNF (Thermo Fisher Scientific, 450-02) and 1 µg/ml laminin (Thermo Fisher Scientific, #23-017-015). Cells were subjected to a partial media change every week.

CRISPRi screening

For each genome-wide sub-library and each lysosomal pH sub-library screen, 45 million iPSCs in 3x T150s were infected with lentivirus as an MOI of ~0.3 and after with puromycin after 48 hours. Cells were selected for 5 days prior to differentiation. iPSCs were then differentiated described and plated on 6x 10-cm PEI-coated dishes at a density of 10 million cells per plate. After two weeks, cells were dissociated using the papain dissociation system (Worthington Biochemical Corporation, 9035-81-1). After dissociation, cells triturated 15 times with a 5 ml serological and filtered through a 40μm cell strainer and pelleted at 200xg for 10 minutes. Cells were washed once in neuronal media, and resuspended in FACS buffer (2% FBS, 1 mM EDTA, and 25 mM HEPES in dPBS) and kept on ice until sorting. After sorting, cells were pelleted at 200×g for 10 minutes, the supernatant was removed, and the pellet was frozen at −20**.** Genomic DNA was extracted with the NucleoSpin Blood S kit. sgRNA cassettes were amplified pooled and sequenced as described [49]. Sequencing was analyzed as described for each sub-library [49]

Screen analysis

Primary screens were analyzed using crispr_screen as previously described [80]. Briefly, raw sequencing reads were cropped and aligned to the protospacer sequences in our libraries using 2FAST2Q [81]. Aligned sgRNA counts were analyzed using an updated MAGeCK-iNC pipeline [49] that uses a negative binomial distribution (https://noamteyssier.github.io/crispr_screen). Phenotypes and p-values for each gene were calculated and hit genes were called based on an FDR of 0.1. Hits were then combined, and gene set enrichment analysis was performed using ENRICHR [82–84].

pH sub-library cloning

A pool of sgRNA-containing oligonucleotides of our top screen hits were synthesized by Twist Bioscience and cloned into an sgRNA expression vector as previously described [50].

iPSC cell line engineering

Genome editing of human KOLF2.1J was performed as described previously [49]. Briefly, the donor plasmid, CLYBL-TO-hNGN2-BSD-mApple (Addgene # 124229), was used to integrate a doxycycline-inducible human NGN2 transgene for neuronal differentiation into the CLYBL safe harbour locus. On the day of transfection, 2.5×10^5 cells were plated per well in Stemflex containing 10μM Y-27632. Ribonucleoprotein (RNP) complexes of sgRNA and HiFi Cas9 nuclease were prepared and combined with 500 ng of donor DNA and 100 ng of pCE-mp53DD plasmid (Addgene, #41856). The mixture was delivered to cells using Lipofectamine™ Stem Transfection Reagent (Thermo Fisher Scientific, STEM00001). The day after transfection, cells were plated by serial dilution for clonal expansion. Antibiotic selection was applied 48-72 hours post-transfection, and floxed mApple and BSD were removed with TAT-Cre Recombinase (MilliporeSigma, SCR508).

Two monoclonal PQLC2 -/- iPSC lines were generated in the background of doxycycline inducible NGN2 KOLF2.1J iPSC [66] using the CRISPR-Cas9 gene editing system. We designed a PQLC2 sgRNA targeting exon 3 (5'-AGCCTACAAGACGGGCAACA-3') using CRISPOR [85] and ligated into the plasmid PX459 as previously described [86]. Plasmids were transfected into 2.5×10^6 iPSCs in a 6 well plate using Lipofectamine STEM. After 48 hours 2μg/ml puromycin was added to select for transfected cells and maintained in puro for 48 hours. Cells were diluted for clonal expansion and genotyping. DNA was collected from clones using the DNeasy Blood and Tissue kit (Qiagen, 69504), and gDNA was amplified using primers

upstream and downstream of sgRNA target (5'- GTCCCCTATAAGGCGGCATC -3', 5'-CAGGGTGAAGCAGGGTTAGG -3'). PCR product was sequenced (Elim Biopharm) and assessed for indels using ICE analysis (EditCo).

Lysosome assays

Cells were plated on eight well chamber slides (Ibidi, 80806) coated with PEI/Laminin at a density of $2.5x10^5$ cells per chamber. For FIRE-pHLy measurement of lysosomal pH, FIRE-pHLy expressing cells were fixed on day 14 in 2% PFA. Fixed cells were washed twice with DPBS and imaged.

For dextran-conjugate pH measurement, 125 ug/ml Oregon Green-488 Dextran (Thermo Fischer Scientific, D7170) and 20 µg/ml CF555-dextran (Biotium, 80112) were added to neuronal media and incubated overnight. The following morning, the cells were gently washed with fresh, warmed neuronal media five times and then the cells were incubated in fresh media for four hours. Dextran assays were imaged live, and media was exchanged to live cell imaging media which consisted of Hibernate-A low fluorescence media (Thermo Fischer Scientific, NC0442869) supplemented with 0.5X N2, 1X B27, 1 µg/ml BDNF, and 1 µg/ml NT-3. Cells were maintained at 37°C using a humidified incubator chamber.

For lysosomal activity assays: DQ Red BSA (Thermo Fisher Scientific, D12051) was added at 50 µg/ml in neuronal media, and incubated for four hours, Pepstatin A, BODIPY™ FL Conjugate (Thermo Fisher Scientific, P12271) was added at 1 µM for one hour, or Magic Red Fluorescent Cathepsin B Assay Kit (Antibodies Inc, 938) was added at a 1:250 dilution in neuronal media for 30 minutes. After incubation, cells were gently washed five times and imaged in live cell imaging media.

Microscopy and image analysis

Cells were plated on eight well chamber slides (Ibidi, 80806) coated with PEI/Laminin at a density of $2.5x10^5$ cells per chamber. For FIRE-pHLy measurements, cells were fixed in 2% PFA for 15 minutes and washed twice in DPBS. For dextran and enzyme activity measurements, Imaging was done using an inverted confocal line-scanning microscope (DMi8 CS Bino, Leica Microsystems Inc., Wetzlar, Germany) with either a 20x/ air objective, 40x oil-immersion objective or a 63×/1.40 oil-immersion objective lens. Fluorescence images were acquired with sequential scanning between frames on the LAS X SP8 Control Software system using preset channel settings. Randomly imaged fields were processed (background subtraction, thresholding), and lysosomal pH ratios were calculated using a Cellprofiler pipeline [87]. Briefly, puncta were segmented for pH insensitive fluorescence (mCherry or CF555) and used as a mask to measure both the pH sensitive and insensitive signal per puncta. The ratio for each puncta was taken and averaged to generate an average ratio per image.

PQLC2 plasmid cloning

Wild-type PQLC2 was ordered codon-optimized from Twist Bioscience. This codon optimized gene was inserted into pLenti PGK Blast DEST (w524-1) by Gibson Assembly (New England Biolabs, E5510S). PQLC2 mutants were generated by PCR of this plasmid to generate DNA fragments with our intended mutation and assembled using Gibson Assembly. For HEK293FT overexpression, PQLC2 was cloned into pLenti CMV Blast DEST (706-1) by Gibson Assembly.

qPCR

To check knockdown of *PQLC2,* RNA was extracted from day 14 iNeurons using the RNeasy mini kit (QIAGEN, 74104) per the manufacter's protocol. xtracted mRNA was converted to cDNA by PCR using SuperScript III Reverse Transcriptase (Invitrogen, 18080-044). qPCR was

performed using standard techniques as previously described [88]. cDNA was amplified using 1x Platinum Superfi II Mastermix (Thermo Fisher Scientific, 12368010) with 1x Evagreen dye (Biotium, 31000) at a 1x concentration and ROX Reference Dye 25 uM (Biotium, 29052) at 0.5 uM concentration. Primers used for PQLC2 mRNA were (5'- gcctgggcttgatctccatt-3', 5'-cacagccgtgtaggtctgc-3').

2.5 Figures

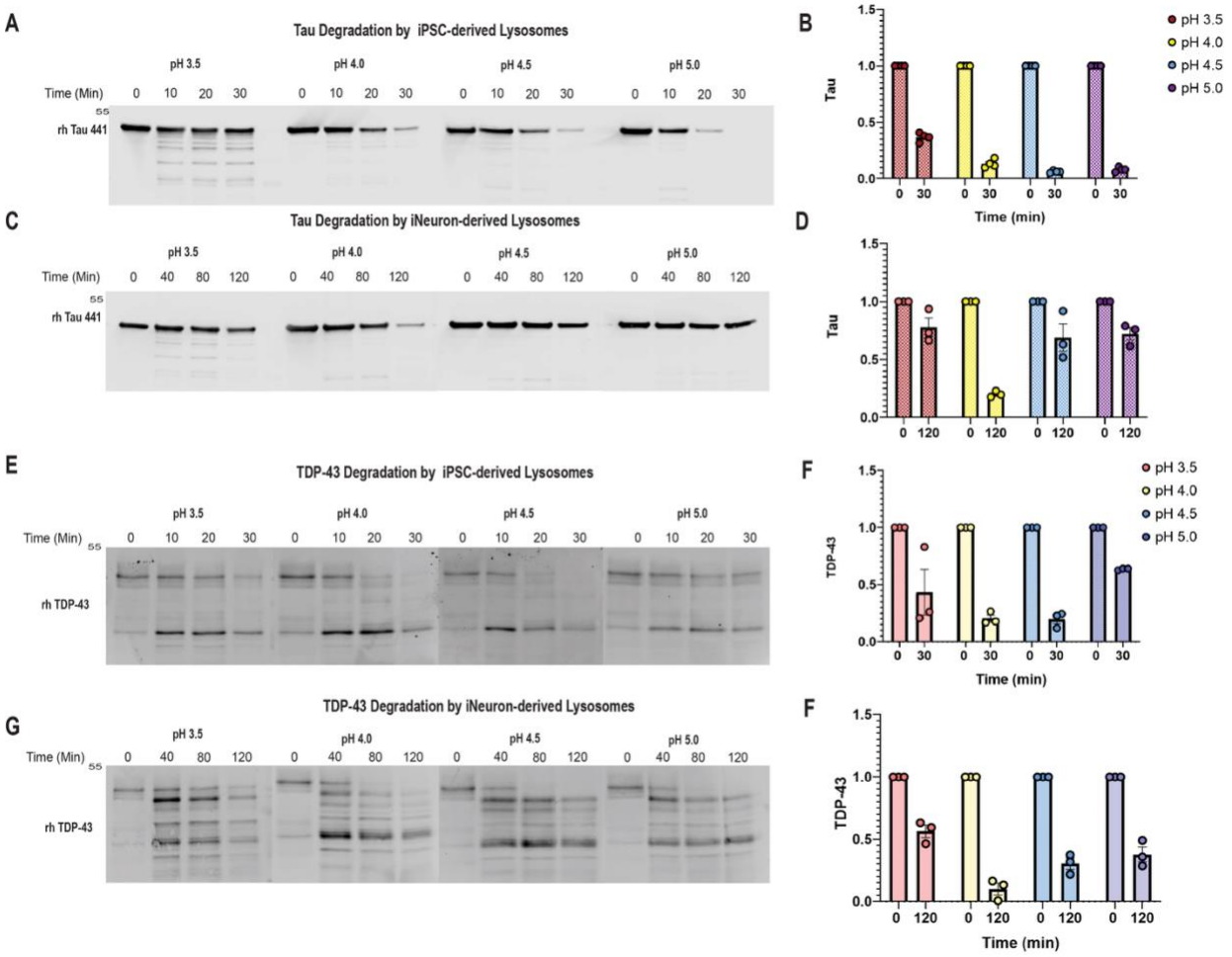

Figure 2.5.1 Neuronal lysosomes exhibit a highly pH-dependent substrate activity profile with a particularly narrow pH range of activity for tau degradation.

A. Western blots of recombinant full-length human tau-441 proteolysis by iPSC-derived lysosomes over 30 minutes in vitro at pHs 3.5, 4.0, 4.5, and 5.0. **B**. Quantification of time points 0 and 30 minutes from the Western blots shown in A **C**. Western blots of recombinant full-length human tau-441 proteolysis by iNeuron-derived lysosomes over 120 minutes in vitro at pHs 3.5, 4.0, 4.5, and 5.0. **D**. Quantification of time points 0 and 120 minutes from the Western blots shown in C. **E.** Western blots of recombinant full-length human TDP-43 proteolysis by iPSC-derived lysosomes over 30 minutes in vitro at pHs 3.5, 4.0, 4.5, and 5.0. **F**. Quantification of time points 0 and 30 minutes from the Western blots shown in E. **G**. Western blots of recombinant full-length human TDP-43 proteolysis by iNeuron-derived lysosomes over 120 minutes in vitro at pHs 3.5, 4.0, 4.5, and 5.0. **H.** Quantification of time points 0 and 120 minutes from the Western blots shown in G.

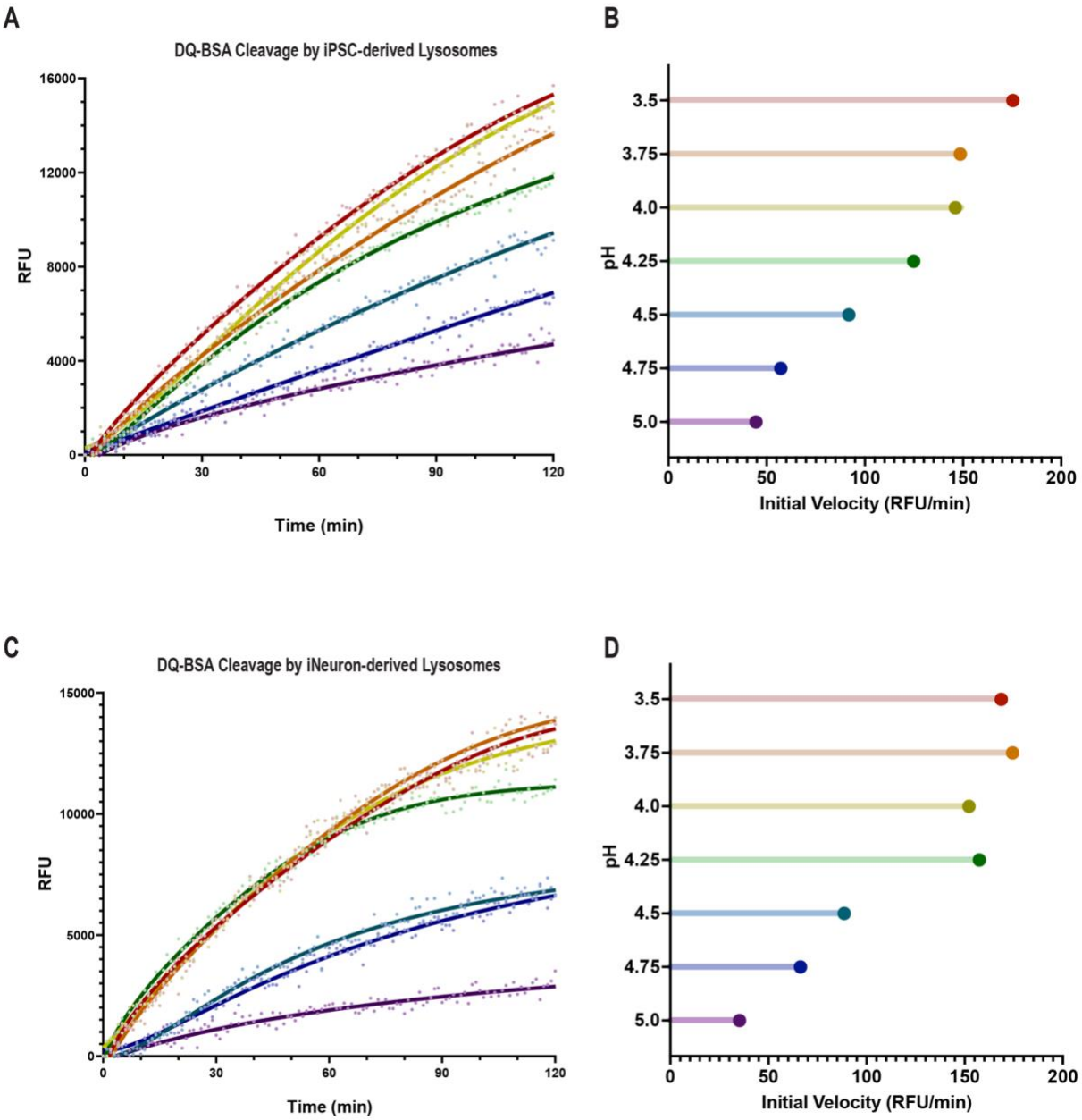

Figure 2.5.2 Neuronal lysosomes exhibit a highly pH-dependent substrate activity profile for TDP-43 degradation and a pH optimum that is narrower than iPSC-derived lysosomes.

A. Activity assay measuring cleavage of a fluorogenic DQ-BSA in the presence of iPSC-derived lysosomes at different pHs. B. Initial velocity (RFU/min) of the activity assays shown in A. C. Activity assay measuring cleavage of a fluorogenic DQ-BSA in the presence of iNeuron-derived lysosomes at different pHs. D. Initial velocity (RFU/min) of the activity assays shown in C

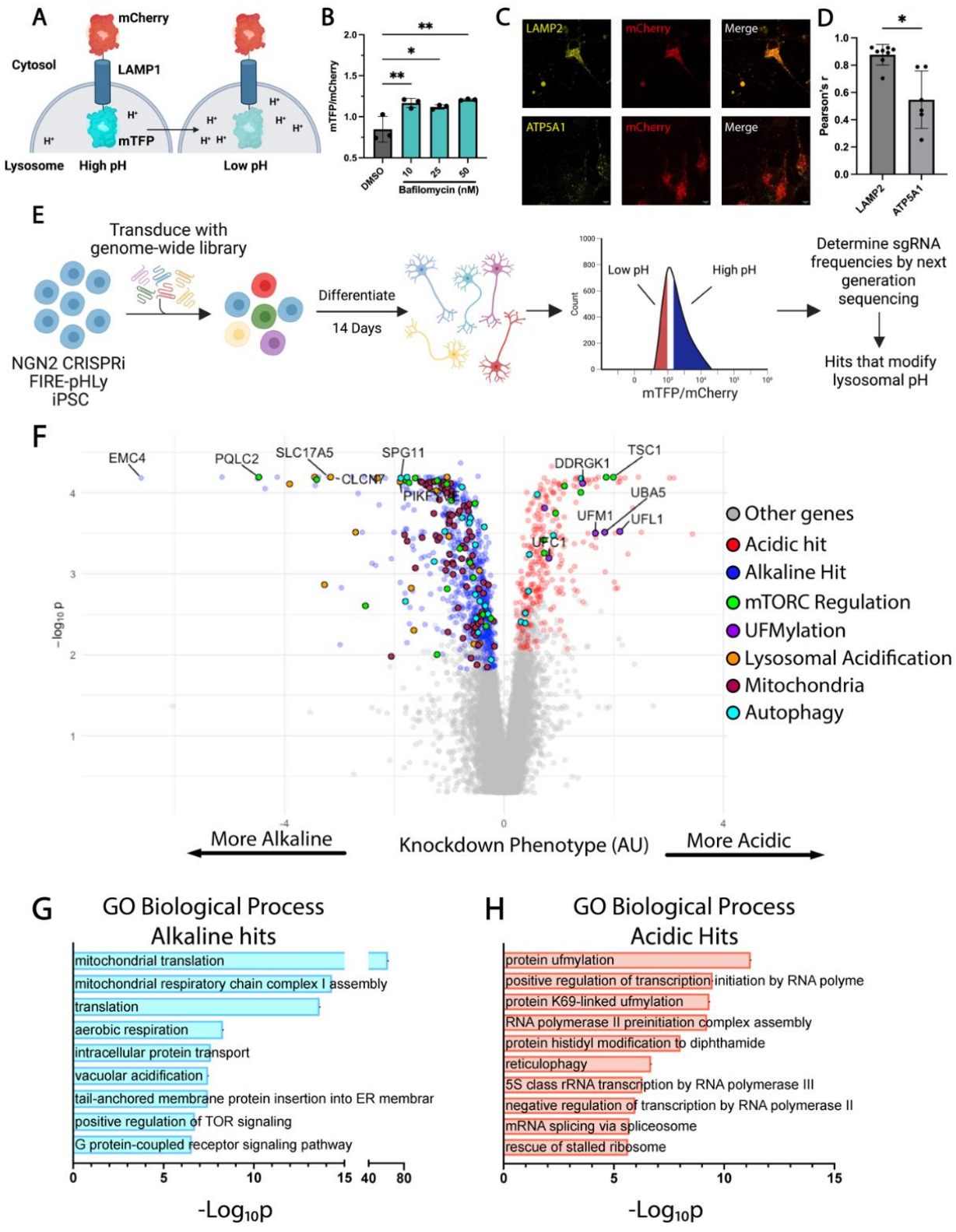

Figure 2.5.3 Genome wide screen for lysosomal pH modifiers in human neurons

(Figure caption continued on the next page.)

(Figure caption continued from the previous page.)
A. Schematic of genetically encoded lysosomal pH reporter, FIRE-pHLy B. Overnight incubation with 10, 25 or 50 nM Bafilomycin-A1 increases mTFP/mCherry ratio indicating increased lysosomal pH in KOLF2.1J neurons C. Representative images of neuronally expressed FIRE-pHLy colocalized with LAMP2 positive organelles in KOLF2.1J neurons and not ATP5A1 (mitochondria) D. Pearson's r correlations of LAMP2:mCherry and ATP5A1:mCherry n=1-2 wells from 4 independent coverslips demonstrating strong colocalization with lysosomes
E. Schematic of neuronal lysosomal pH screen, iPSCs expressing FIRE-pHLy and NGN2 were transduced with pooled libraries targeting the coding genome. iPSCs were differentiated into neurons for two weeks prior to dissociation and FACS sorting. The thirty percent corresponding to high (blue) or low lysosomal pH (red) were separated by FACS. Genomic DNA was isolated and the sgRNA was sequenced by next generation sequencing F. Volcano plot of hit genes from genome-wide screen. Phenotype (normalized log2 ratio of counts in the mTFP:mCherry high versus mTFP:mCherry low populations), is plotted versus the negative log10 of the P-value, calculated with a Mann-Whitney U-test. Acidic hits are in red, and alkaline hits are in blue G. GO biological process terms for Alkaline pH hits H. GO biological process terms for acidic pH hits * $p < 0.05$, ** < 0.01, *** < 0.001.

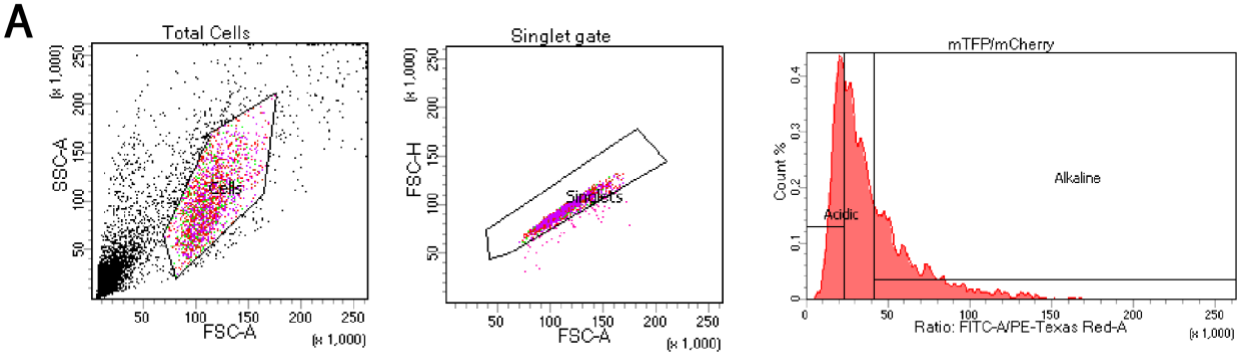

Figure 2.5.4 FACS Gating for FIRE-pHLy iNeurons

A. Representative gating strategy for sorting high mTFP/mCherry and low mTFP/mCherry populations of cells

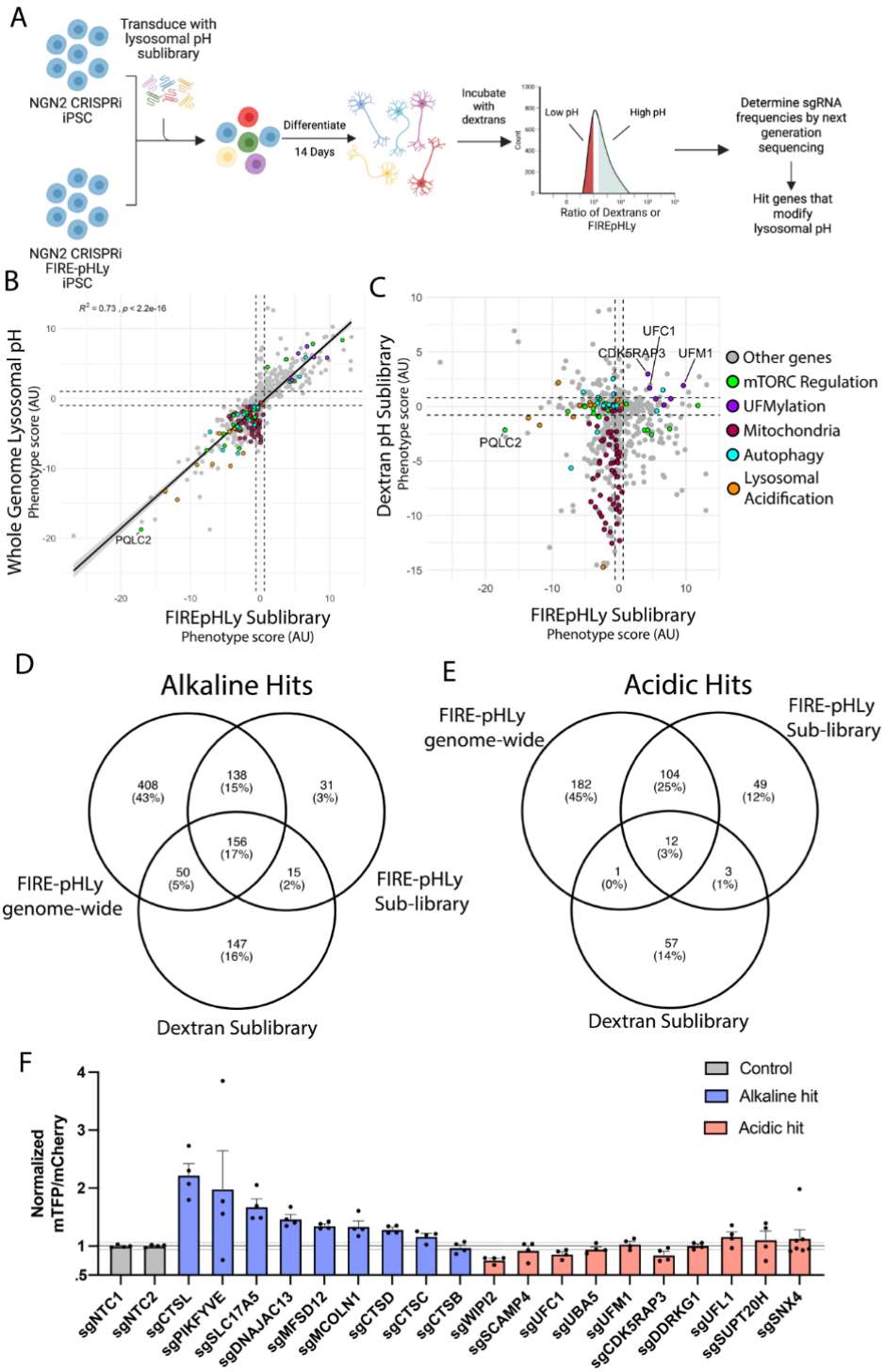

Figure 2.5.5 Validation of whole genome lysosomal pH screen demonstrates robustness of alkaline hits

A. Sublibrary iNeuron screen schematic. Cells expressing FIRE-pHLy or no sensor were transduced with the pH sgRNA sublibrary and differentiated into neurons for two weeks. For

(Figure caption continued on the next page.)

(Figure caption continued from the previous page.)
dextran-based lysosomal pH measurement, cells were stained with Oregon Green 488-dextran and CF555-Dextran overnight and chased to the lysosome with a 4 hour incubation in fresh media. Cells with either FIRE-pHLy or the dextrans were dissociated and high and low lysosome pH fractions were collected by FACS **B**. Correlation between sub-library FIRE-pHLy screen phenotype score and whole genome screen phenotype score (Pearson's r = 0.73) **C.** Comparison between FIRE-pHLy phenotype score and dextran based sub-library screen phenotype score **D.** Overlap between alkalinizing hit genes in whole genome and two sub-library screens **E.** Overlap between acidic hit genes across all three lysosomal pH screens **F**. Imaging validation of select hit genes using individually cloned sgRNAs. Mean of 4 biological replicates, blue bars were alkaline hits in our initial screen, red bars were acidic hits. Error bars are standard deviation. Dashed line is 3-fold standard deviation of the control mTFP/mCherry ratios.

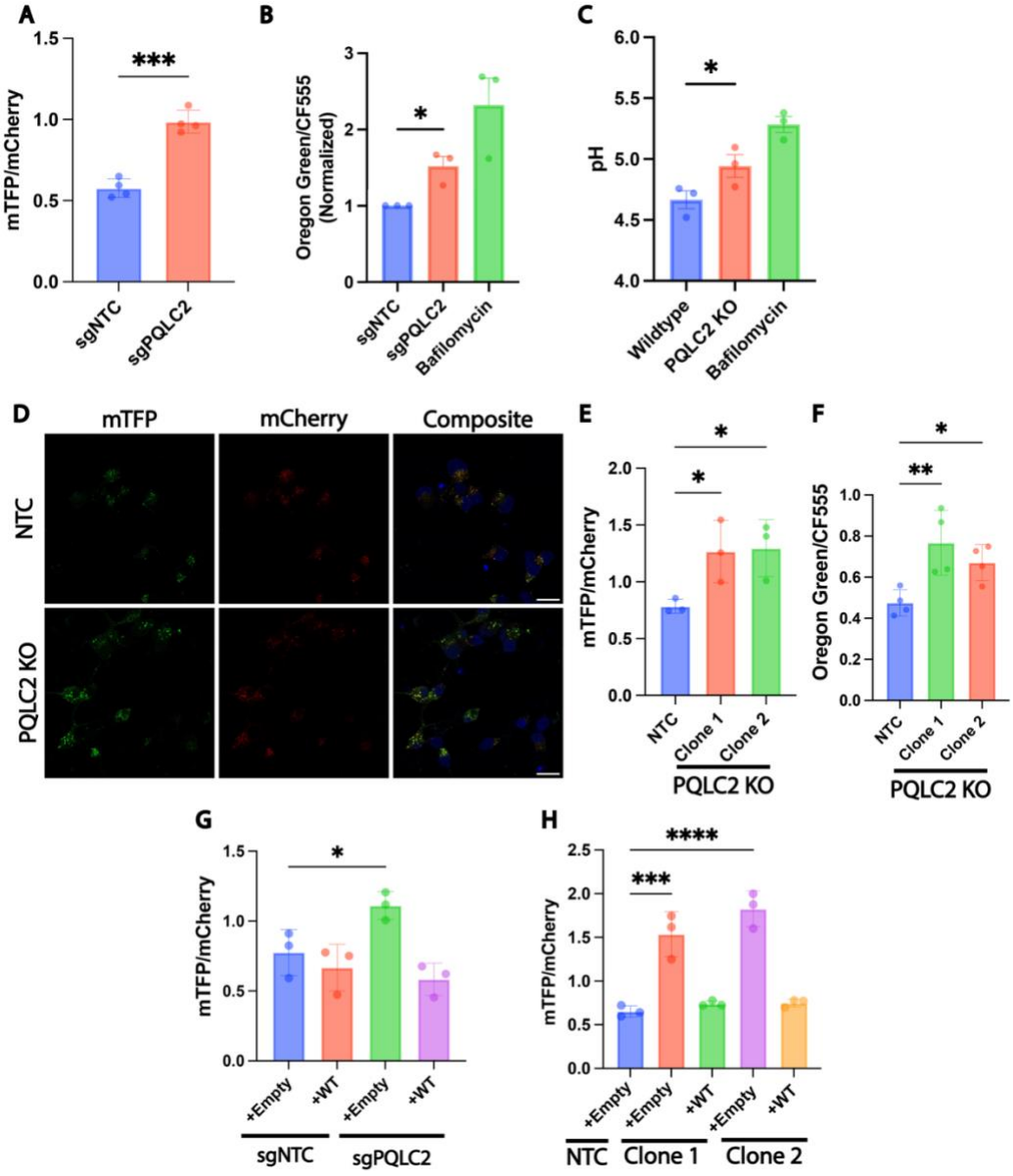

Figure 2.5.6 PQLC2 is required for maintenance of lysosomal pH homeostasis

A. Day 14 iNeurons with *PQLC2* knockdown by CRISPRi increases mTFP/mCherry ratio n=4 independent experiments **B**. Day 14 iNeurons with *PQLC2* knockdown by CRISPRi increases Oregon Green/CF555 ratio n=3 independent experiments **C.** Absolute lysosomal pH as measured by Oregon Green-488 dextran is increased in HEK293FT PQLC2 knockout cells n=3 independent experiments **D.** Representative images of PQLC2 knockout iNeurons scalebar = 20 µm **E.** PQLC2 knockout iNeurons show increased mTFP/mCherry ratio in two independent clones n=3 independent experiments **F.** PQLC2 knockout iNeurons have increased oregon green/CF555 ratio in two independent PQLC2 knockout clones n=4 independent experiments
(Figure caption continued on the next page.)

(Figure caption continued from the previous page.)
G. Stable expression of PQLC2 rescues lysosomal pH phenotype in CRISPRi PQLC2 knockdown cell line n=3 independent experiments **H.** Stable expression of PQLC2 in iNeurons rescues lysosomal pH phenotype in two PQLC2 knockout clones n=3 *$p < 0.05$, **$p < 0.01$, or ***$p < 0.001$

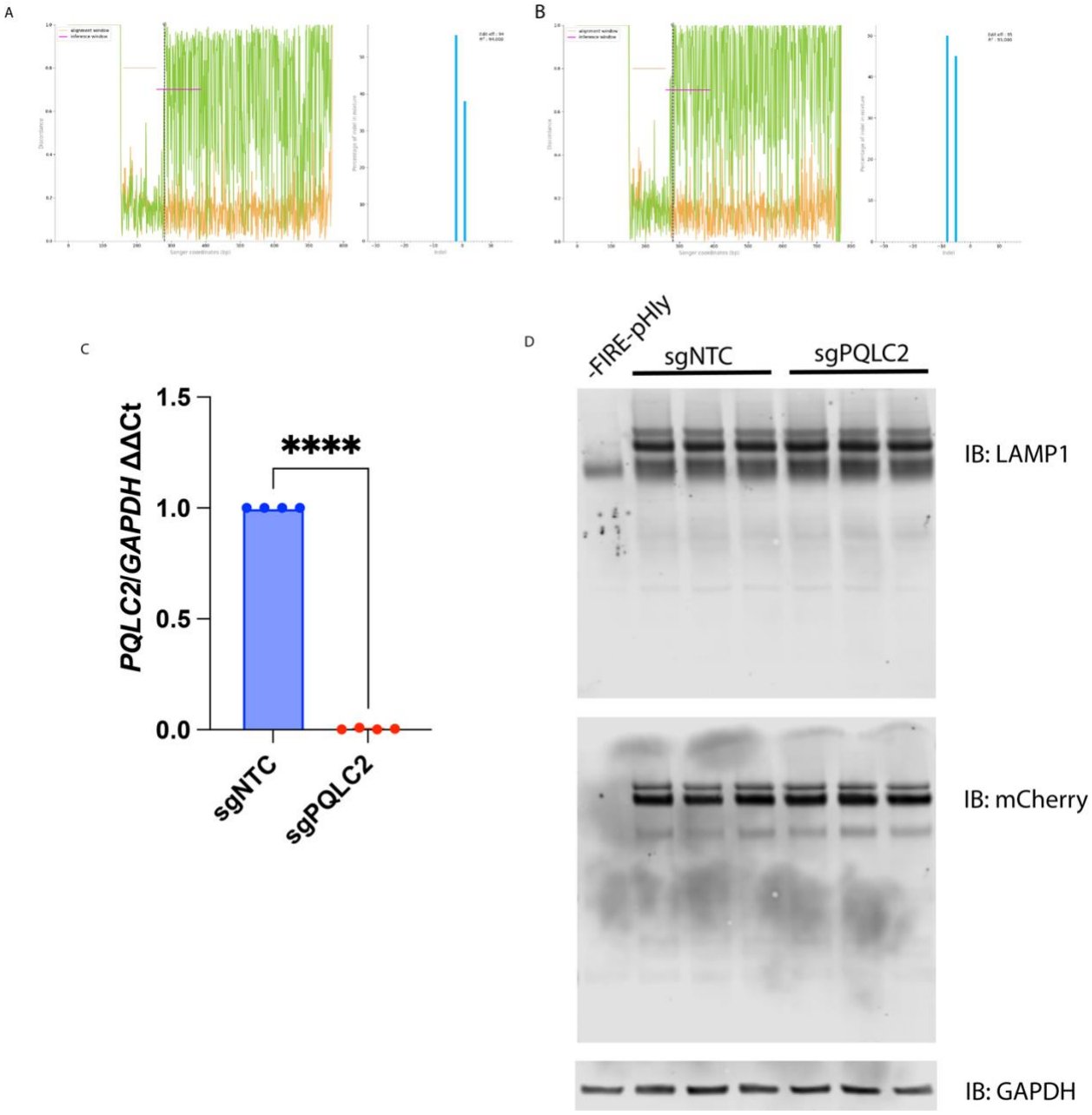

Figure 2.5.7 Validation of PQLC2 iPSC lines

A, B. ICE analysis for both PQLC2 knockout iPSC clones showing high probability of a double frameshift C. Relative mRNA levels of PQLC2 in CRISPRi PQLC2 knockdown iNeurons $p<0.0001$ D. Western blot of CRISPRi PQLC2 neurons demonstrating PQLC2 knockdown maintains normal expression of FIRE-pHLy

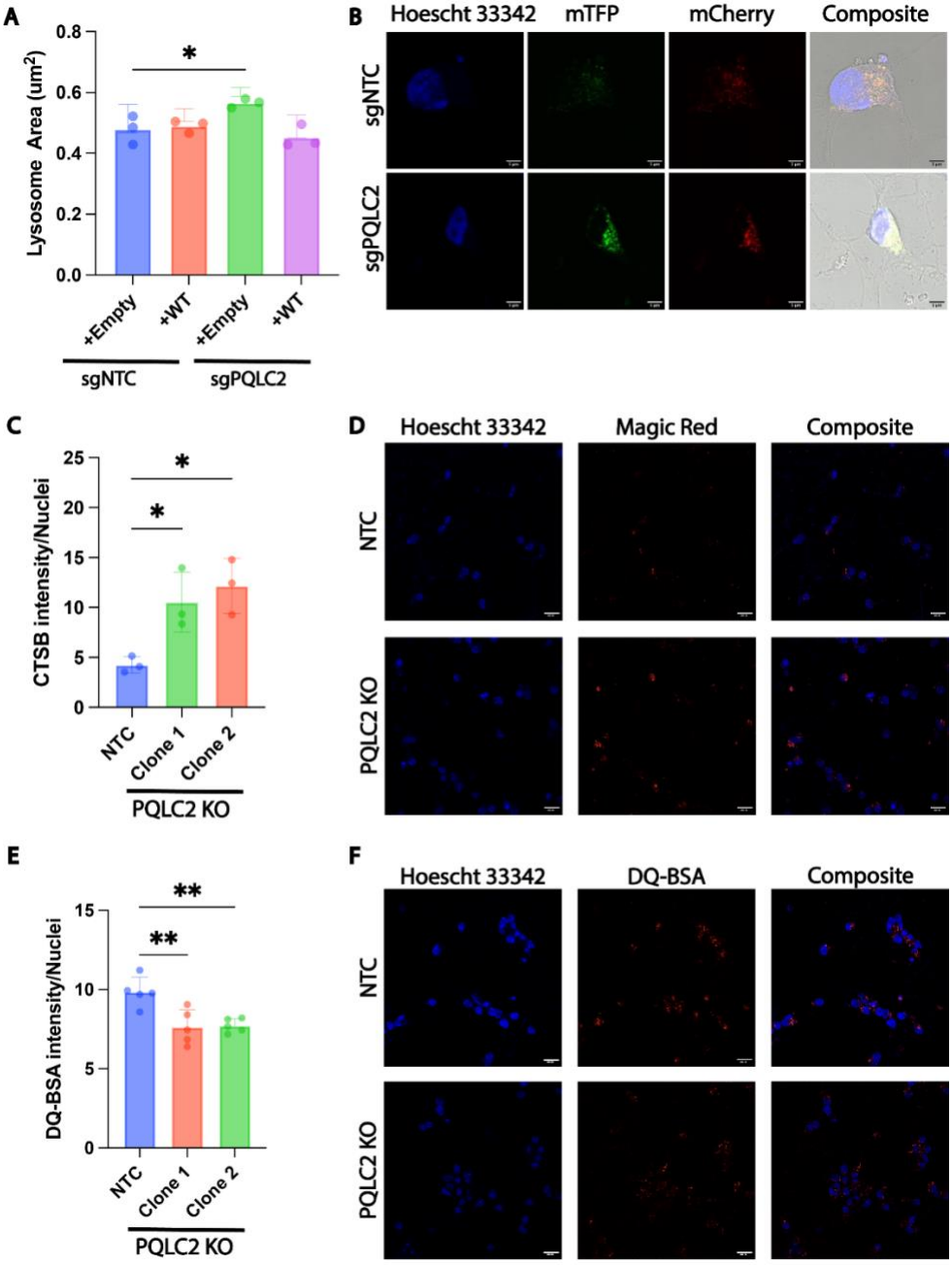

Figure 2.5.8 Loss of PQLC2 causes lysosomal dysfunction

A. CRISPRi knockdown of PQLC2 increases lysosome size that is rescued by re-expression of PQLC2 (n=3) **B.** Representative images increased lysosome size in PQLC2 knockdown neurons **C.** CTSB Magic red staining shows increased CTSB substrate hydrolysis in day 14 PQLC2 knockout iNeurons **D.** Representative images of CTSB magic red staining in control of PQLC2 knockout neurons

(Figure caption continued on the next page.)

(Figure caption continued from the previous page.)
E. DQ-BSA intensity is decreased in day 14 PQLC2 knockout iNeurons compared to control cells **F.** Representative image of DQ-BSA staining in PQLC2 knockout iNeurons $*p < 0.05$, or $**p < 0.01$

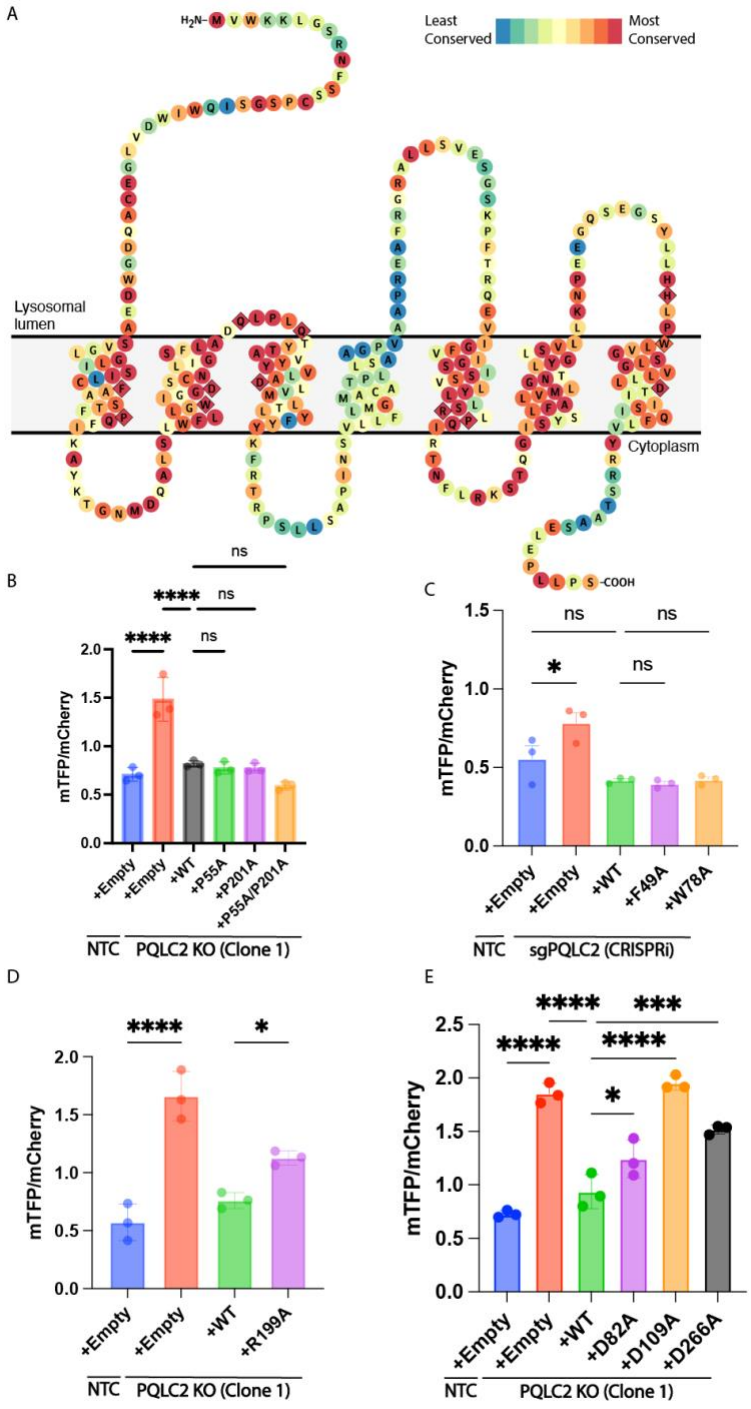

Figure 2.5.9 Charged residues within the transmembrane domain of PQLC2 are required for lysosomal pH homeostasis
(Figure caption continued on the next page.)

(Figure caption continued from the previous page.)
A. PQLC2 protein schematic highlighted by conservation score with mutants tested ringed in diamonds **B.** Expression of either PQLC2^{P55L}, PQLC2^{P201L}, PQLC2$^{P55L/P201L}$ are all sufficient to rescue lysosomal pH in Day 14 PQLC2 knockout iNeurons by FIRE-pHLy signal. **C.** Two known mutants for CSW binding, PQLC2^{F49A} PQLC2^{W78A}, restore normal lysosomal pH in day 14 PQLC2 knockout iNeurons. **D.** Re-expression of pathogenic PQLC2^{R199Q} fails to fully rescue lysosomal pH in Day 14 PQLC2 knockout iNeurons **E.** Expression of either PQLC2^{D82A}, PQLC2^{D109A}, PQLC2^{D266A}, fails to rescue lysosomal pH in day 14 PQLC2 knockout iNeurons
*$p < 0.05$, **$p < 0.01$, or ***$p<0.001$

Chapter 3: Discussion

3.1 Summary

We have reported the first comprehensive screen for modifiers of neuronal lysosomal pH, and highlight that both mitochondria and protein UFMylation as robust, previously unreported modifiers of lysosomal pH. These data are a resource for understanding how lysosomal pH is regulated and represent potential novel targets for the treatment of neurodegenerative disease. A prior effort to identify lysosomal pH modifiers identified 15 pH modifying genes in the genome using LysoSensor [73], and we expand on this work with a more comprehensive profiling of lysosomal pH modifiers. We believe the differences in results are in part due to methodology, highlighting the improvement genetically encoded pH sensors have over prior methods for large-scale screens.

We discovered that PQLC2, a lysosomal cationic amino acid exporter, regulates lysosomal pH through the export of charged amino acids, and demonstrate through multiple methodologies that loss of PQLC2 results in a large increase in lysosomal pH, and this increase can be rescued by re-expression of PQLC2. Additionally, we find the aspartic acids within the transmembrane domain of PQLC2 to be critical for lysosomal pH homeostasis, and mutating these charged residues to neutral residues fails to rescue lysosomal pH. We also show that loss of PQLC2 bears the hallmarks of lysosomal storage diseases with disrupted protein degradation, enlarged lysosomes and dysregulated pH. This work stands in contrast to prior literature that has proposed that PQLC2 regulates lysosomal pH through an undefined interaction with the V-ATPase [77] and highlights another cationic amino acid export as capable of modifying lysosomal pH similar to neutral amino acids through SLC7A11 [20].

Our work highlights the complexity of lysosome biology, and lysosomal pH regulation. We have identified and validated the mechanism behind a strong modifier of lysosomal pH, but our data represents a resource for further understanding of lysosomal pH regulation, as well as advance our understanding of a novel export pathway regulating lysosomal pH.

3.2 Future Directions

Two questions remain from our work: 1) Can PQLC2 be targeted to lower lysosomal pH and 2) Are any of our lysosomal pH modifying hit genes neuron intrinsic? Both these questions would represent an important step in the treatment of neurodegenerative disease. PQLC2 exports cationic amino acids from the lysosome [63], and loss of PQLC2 causes an accumulation of its substrates [64], we hypothesize that activating PQLC2 to decrease lysosomal cationic amino acid levels may serve as a mechanism to decrease lysosomal pH in the short term. Targeting PQLC2 to activate transport of cationic amino acids could potentially act as both a tool compound for lysosomal acidification and be a potential therapeutic to decrease lysosomal pH and increase degradation of lysosomal substrates.

Additionally, given the associations between aging, neurodegenerative disease and lysosomal pH [27, 30, 37, 38], identifying neuron intrinsic mechanisms of lysosomal pH regulation would help in the treatment of neurodegenerative disease. We believe that targeting lysosomal pH represents a possible disease-modifying treatment in neurodegenerative disease. The link between mitochondrial health, ATP levels and lysosomal pH we identified warrants further follow up given the reliance of neurons on mitochondria and cellular respiration [89]. There is a large body of evidence as well that mitochondrial dysfunction can be a cell-autonomous driver of neuronal death in Parkinson's disease [90], and might be required for

efficient neuronal lysosomal pH homeostasis as other cell types are able to rely on glycolysis. This represents an interesting, potential neuron intrinsic finding that warrants further follow-up, and may possibly serve as the linkage between mitochondrial dysfunction and lysosomal dysfunction seen in neurodegeneration.

References

[1] Klaips, C. L.; Jayaraj, G. G.; Hartl, F. U. Pathways of Cellular Proteostasis in Aging and Disease. *J. Cell Biol.*, **2017**, *217* (1), 51–63. https://doi.org/10.1083/jcb.201709072.

[2] Lamark, T.; Johansen, T. Aggrephagy: Selective Disposal of Protein Aggregates by Macroautophagy. *Int. J. Cell Biol.*, **2012**, *2012*, 736905. https://doi.org/10.1155/2012/736905.

[3] Anding, A. L.; Baehrecke, E. H. Cleaning House: Selective Autophagy of Organelles. *Dev. Cell*, **2017**, *41* (1), 10–22. https://doi.org/10.1016/j.devcel.2017.02.016.

[4] Graves, A. R.; Curran, P. K.; Smith, C. L.; Mindell, J. A. The Cl-/H+ Antiporter ClC-7 Is the Primary Chloride Permeation Pathway in Lysosomes. *Nature*, **2008**, *453* (7196), 788–792. https://doi.org/10.1038/nature06907.

[5] Mindell, J. A. Lysosomal Acidification Mechanisms. *Annu. Rev. Physiol.*, **2012**, *74*, 69–86. https://doi.org/10.1146/annurev-physiol-012110-142317.

[6] Hu, M.; Li, P.; Wang, C.; Feng, X.; Geng, Q.; Chen, W.; Marthi, M.; Zhang, W.; Gao, C.; Reid, W.; et al. Parkinson's Disease-Risk Protein TMEM175 Is a Proton-Activated Proton Channel in Lysosomes. *Cell*, **2022**, *185* (13), 2292-2308.e20. https://doi.org/10.1016/j.cell.2022.05.021.

[7] Cao, Q.; Yang, Y.; Zhong, X. Z.; Dong, X.-P. The Lysosomal Ca2+ Release Channel TRPML1 Regulates Lysosome Size by Activating Calmodulin. *J. Biol. Chem.*, **2017**, *292* (20), 8424–8435. https://doi.org/10.1074/jbc.M116.772160.

[8] Wallings, R. L.; Humble, S. W.; Ward, M. E.; Wade-Martins, R. Lysosomal Dysfunction at the Centre of Parkinson's Disease and Frontotemporal Dementia/Amyotrophic Lateral

Sclerosis. *Trends Neurosci.*, **2019**, *42* (12), 899–912. https://doi.org/10.1016/j.tins.2019.10.002.

[9] Xiong, J.; Zhu, M. X. Regulation of Lysosomal Ion Homeostasis by Channels and Transporters. *Sci. China Life Sci.*, **2016**, *59* (8), 777–791. https://doi.org/10.1007/s11427-016-5090-x.

[10] Forgac, M. Vacuolar ATPases: Rotary Proton Pumps in Physiology and Pathophysiology. *Nat. Rev. Mol. Cell Biol.*, **2007**, *8* (11), 917–929. https://doi.org/10.1038/nrm2272.

[11] Li, S. C.; Diakov, T. T.; Xu, T.; Tarsio, M.; Zhu, W.; Couoh-Cardel, S.; Weisman, L. S.; Kane, P. M. The Signaling Lipid PI(3,5)P2 Stabilizes V1–Vo Sector Interactions and Activates the V-ATPase. *Mol. Biol. Cell*, **2014**, *25* (8), 1251–1262. https://doi.org/10.1091/mbc.e13-10-0563.

[12] Smardon, A. M.; Tarsio, M.; Kane, P. M. The RAVE Complex Is Essential for Stable Assembly of the Yeast V-ATPase *. *J. Biol. Chem.*, **2002**, *277* (16), 13831–13839. https://doi.org/10.1074/jbc.M200682200.

[13] Tabke, K.; Albertmelcher, A.; Vitavska, O.; Huss, M.; Schmitz, H.-P.; Wieczorek, H. Reversible Disassembly of the Yeast V-ATPase Revisited under in Vivo Conditions. *Biochem. J.*, **2014**, *462* (1), 185–197. https://doi.org/10.1042/BJ20131293.

[14] Kane, P. M. Disassembly and Reassembly of the Yeast Vacuolar H(+)-ATPase in Vivo. *J. Biol. Chem.*, **1995**, *270* (28), 17025–17032.

[15] Ratto, E.; Chowdhury, S. R.; Siefert, N. S.; Schneider, M.; Wittmann, M.; Helm, D.; Palm, W. Direct Control of Lysosomal Catabolic Activity by mTORC1 through Regulation of V-ATPase Assembly. *Nat. Commun.*, **2022**, *13* (1), 4848. https://doi.org/10.1038/s41467-022-32515-6.

[16] Zoncu, R.; Bar-Peled, L.; Efeyan, A.; Wang, S.; Sancak, Y.; Sabatini, D. M. mTORC1 Senses Lysosomal Amino Acids through an Inside-out Mechanism That Requires the Vacuolar H+-ATPase. *Science*, **2011**, *334* (6056), 678–683. https://doi.org/10.1126/science.1207056.

[17] Shao, E.; Forgac, M. Involvement of the Nonhomologous Region of Subunit A of the Yeast V-ATPase in Coupling and in Vivo Dissociation *. *J. Biol. Chem.*, **2004**, *279* (47), 48663–48670. https://doi.org/10.1074/jbc.M408278200.

[18] Yuan, Y.; Jaślan, D.; Rahman, T.; Bolsover, S. R.; Arige, V.; Wagner, L. E.; Abrahamian, C.; Tang, R.; Keller, M.; Hartmann, J.; et al. Segregated Cation Flux by TPC2 Biases Ca2+ Signaling through Lysosomes. *Nat. Commun.*, **2022**, *13* (1), 4481. https://doi.org/10.1038/s41467-022-31959-0.

[19] Guo, J.; Zeng, W.; Jiang, Y. Tuning the Ion Selectivity of Two-Pore Channels. *Proc. Natl. Acad. Sci. U. S. A.*, **2017**, *114* (5), 1009–1014. https://doi.org/10.1073/pnas.1616191114.

[20] Zhou, N.; Chen, J.; Hu, M.; Wen, N.; Cai, W.; Li, P.; Zhao, L.; Meng, Y.; Zhao, D.; Yang, X.; et al. SLC7A11 Is an Unconventional H+ Transporter in Lysosomes. *Cell*, **2025**, *188* (13), 3441-3458.e25. https://doi.org/10.1016/j.cell.2025.04.004.

[21] Cang, C.; Aranda, K.; Seo, Y.; Gasnier, B.; Ren, D. TMEM175 Is an Organelle K(+) Channel Regulating Lysosomal Function. *Cell*, **2015**, *162* (5), 1101–1112. https://doi.org/10.1016/j.cell.2015.08.002.

[22] Steinmetz, J. D.; Seeher, K. M.; Schiess, N.; Nichols, E.; Cao, B.; Servili, C.; Cavallera, V.; Cousin, E.; Hagins, H.; Moberg, M. E.; et al. Global, Regional, and National Burden of Disorders Affecting the Nervous System, 1990–2021: A Systematic Analysis for the Global

Burden of Disease Study 2021. *Lancet Neurol.*, **2024**, *23* (4), 344–381. https://doi.org/10.1016/S1474-4422(24)00038-3.

[23] Vidyadhara, D. J.; Lee, J. E.; Chandra, S. S. Role of the Endolysosomal System in Parkinson's Disease. *J. Neurochem.*, **2019**, *150* (5), 487–506. https://doi.org/10.1111/jnc.14820.

[24] Todd, T. W.; Shao, W.; Zhang, Y.; Petrucelli, L. The Endolysosomal Pathway and ALS/FTD. *Trends Neurosci.*, **2023**, *46* (12), 1025–1041. https://doi.org/10.1016/j.tins.2023.09.004.

[25] Sampognaro, P. J.; Arya, S.; Knudsen, G. M.; Gunderson, E. L.; Sandoval-Perez, A.; Hodul, M.; Bowles, K.; Craik, C. S.; Jacobson, M. P.; Kao, A. W. Mutations in α-Synuclein, TDP-43 and Tau Prolong Protein Half-Life through Diminished Degradation by Lysosomal Proteases. *Mol. Neurodegener.*, **2023**, *18* (1), 29. https://doi.org/10.1186/s13024-023-00621-8.

[26] Kaganovich, D.; Kopito, R.; Frydman, J. Misfolded Proteins Partition between Two Distinct Quality Control Compartments. *Nature*, **2008**, *454* (7208), 1088–1095. https://doi.org/10.1038/nature07195.

[27] Lee, J.-H.; Yu, W. H.; Kumar, A.; Lee, S.; Mohan, P. S.; Peterhoff, C. M.; Wolfe, D. M.; Martinez-Vicente, M.; Massey, A. C.; Sovak, G.; et al. Lysosomal Proteolysis and Autophagy Require Presenilin 1 and Are Disrupted by Alzheimer-Related PS1 Mutations. *Cell*, **2010**, *141* (7), 1146–1158. https://doi.org/10.1016/j.cell.2010.05.008.

[28] Lee, J.-H.; Yang, D.-S.; Goulbourne, C. N.; Im, E.; Stavrides, P.; Pensalfini, A.; Chan, H.; Bouchet-Marquis, C.; Bleiwas, C.; Berg, M. J.; et al. Faulty Autolysosome Acidification in Alzheimer's Disease Mouse Models Induces Autophagic Build-up of Aβ in Neurons,

Yielding Senile Plaques. *Nat. Neurosci.*, **2022**, *25* (6), 688–701. https://doi.org/10.1038/s41593-022-01084-8.

[29] Wolfe, D. M.; Lee, J.; Kumar, A.; Lee, S.; Orenstein, S. J.; Nixon, R. A. Autophagy Failure in Alzheimer's Disease and the Role of Defective Lysosomal Acidification. *Eur. J. Neurosci.*, **2013**, *37* (12), 1949–1961. https://doi.org/10.1111/ejn.12169.

[30] Wallings, R.; Connor-Robson, N.; Wade-Martins, R. LRRK2 Interacts with the Vacuolar-Type H+-ATPase Pump A1 Subunit to Regulate Lysosomal Function. *Hum. Mol. Genet.*, **2019**, *28* (16), 2696–2710. https://doi.org/10.1093/hmg/ddz088.

[31] Logan, T.; Simon, M. J.; Rana, A.; Cherf, G. M.; Srivastava, A.; Davis, S. S.; Low, R. L. Y.; Chiu, C.-L.; Fang, M.; Huang, F.; et al. Rescue of a Lysosomal Storage Disorder Caused by Grn Loss of Function with a Brain Penetrant Progranulin Biologic. *Cell*, **2021**, *184* (18), 4651-4668.e25. https://doi.org/10.1016/j.cell.2021.08.002.

[32] Arotcarena, M.-L.; Soria, F. N.; Cunha, A.; Doudnikoff, E.; Prévot, G.; Daniel, J.; Blanchard-Desce, M.; Barthélémy, P.; Bezard, E.; Crauste-Manciet, S.; et al. Acidic Nanoparticles Protect against α-Synuclein-Induced Neurodegeneration through the Restoration of Lysosomal Function. *Aging Cell*, **2022**, *21* (4), e13584. https://doi.org/10.1111/acel.13584.

[33] Im, E.; Jiang, Y.; Stavrides, P. H.; Darji, S.; Erdjument-Bromage, H.; Neubert, T. A.; Choi, J. Y.; Wegiel, J.; Lee, J.-H.; Nixon, R. A. Lysosomal Dysfunction in Down Syndrome and Alzheimer Mouse Models Is Caused by V-ATPase Inhibition by Tyr682-Phosphorylated APP βCTF. *Sci. Adv.*, *9* (30), eadg1925. https://doi.org/10.1126/sciadv.adg1925.

[34] Klein, Z. A.; Takahashi, H.; Ma, M.; Stagi, M.; Zhou, M.; Lam, T. T.; Strittmatter, S. M. Loss of TMEM106B Ameliorates Lysosomal and Frontotemporal Dementia-Related

Phenotypes in Progranulin-Deficient Mice. *Neuron*, **2017**, *95* (2), 281-296.e6. https://doi.org/10.1016/j.neuron.2017.06.026.

[35] Jiang, Q.; Liu, J.; Huang, S.; Wang, X.-Y.; Chen, X.; Liu, G.-H.; Ye, K.; Song, W.; Masters, C. L.; Wang, J.; et al. Antiageing Strategy for Neurodegenerative Diseases: From Mechanisms to Clinical Advances. *Signal Transduct. Target. Ther.*, **2025**, *10* (1), 76. https://doi.org/10.1038/s41392-025-02145-7.

[36] Barbosa, M. C.; Grosso, R. A.; Fader, C. M. Hallmarks of Aging: An Autophagic Perspective. *Front. Endocrinol.*, **2019**, *9*, 790. https://doi.org/10.3389/fendo.2018.00790.

[37] Hughes, A. L.; Gottschling, D. E. An Early Age Increase in Vacuolar pH Limits Mitochondrial Function and Lifespan in Yeast. *Nature*, **2012**, *492* (7428), 261–265. https://doi.org/10.1038/nature11654.

[38] Sun, Y.; Li, M.; Zhao, D.; Li, X.; Yang, C.; Wang, X. Lysosome Activity Is Modulated by Multiple Longevity Pathways and Is Important for Lifespan Extension in C. Elegans. *eLife*, **2020**, *9*, e55745. https://doi.org/10.7554/eLife.55745.

[39] Lim, C.-Y.; Zoncu, R. The Lysosome as a Command-and-Control Center for Cellular Metabolism. *J. Cell Biol.*, **2016**, *214* (6), 653–664. https://doi.org/10.1083/jcb.201607005.

[40] Srivastava, J.; Barber, D. L.; Jacobson, M. P. Intracellular pH Sensors: Design Principles and Functional Significance. *Physiology*, **2007**, *22* (1), 30–39. https://doi.org/10.1152/physiol.00035.2006.

[41] Settembre, C.; Fraldi, A.; Medina, D. L.; Ballabio, A. Signals from the Lysosome: A Control Centre for Cellular Clearance and Energy Metabolism. *Nat. Rev. Mol. Cell Biol.*, **2013**, *14* (5), 283–296. https://doi.org/10.1038/nrm3565.

[42] Turk, B.; Dolenc, I.; Lenarčič, B.; Križaj, I.; Turk, V.; Bieth, J. G.; Björk, I. Acidic pH as a Physiological Regulator of Human Cathepsin L Activity. *Eur. J. Biochem.*, **1999**, *259* (3), 926–932. https://doi.org/10.1046/j.1432-1327.1999.00145.x.

[43] Dehay, B.; Ramirez, A.; Martinez-Vicente, M.; Perier, C.; Canron, M.-H.; Doudnikoff, E.; Vital, A.; Vila, M.; Klein, C.; Bezard, E. Loss of P-Type ATPase ATP13A2/PARK9 Function Induces General Lysosomal Deficiency and Leads to Parkinson Disease Neurodegeneration. *Proc. Natl. Acad. Sci.*, **2012**, *109* (24), 9611–9616. https://doi.org/10.1073/pnas.1112368109.

[44] Guo, J.; Huang, X.; Dou, L.; Yan, M.; Shen, T.; Tang, W.; Li, J. Aging and Aging-Related Diseases: From Molecular Mechanisms to Interventions and Treatments. *Signal Transduct. Target. Ther.*, **2022**, *7* (1), 391. https://doi.org/10.1038/s41392-022-01251-0.

[45] Canton, J.; Grinstein, S. Chapter 5 - Measuring Lysosomal pH by Fluorescence Microscopy. In *Methods in Cell Biology*; Platt, F., Platt, N., Eds.; Lysosomes and Lysosomal Diseases; Academic Press, 2015; Vol. 126, pp 85–99. https://doi.org/10.1016/bs.mcb.2014.10.021.

[46] Chin, M. Y.; Patwardhan, A. R.; Ang, K.-H.; Wang, A. L.; Alquezar, C.; Welch, M.; Nguyen, P. T.; Grabe, M.; Molofsky, A. V.; Arkin, M. R.; et al. Genetically Encoded, pH-Sensitive mTFP1 Biosensor for Probing Lysosomal pH. *ACS Sens.*, **2021**, *6* (6), 2168–2180. https://doi.org/10.1021/acssensors.0c02318.

[47] Chin, M. Y.; Ang, K.-H.; Davies, J.; Alquezar, C.; Garda, V. G.; Rooney, B.; Leng, K.; Kampmann, M.; Arkin, M. R.; Kao, A. W. Phenotypic Screening Using High-Content Imaging to Identify Lysosomal pH Modulators in a Neuronal Cell Model. *ACS Chem. Neurosci.*, **2022**, *13* (10), 1505–1516. https://doi.org/10.1021/acschemneuro.1c00804.

[48] Abu-Remaileh, M.; Wyant, G. A.; Kim, C.; Laqtom, N. N.; Abbasi, M.; Chan, S. H.; Freinkman, E.; Sabatini, D. M. Lysosomal Metabolomics Reveals V-ATPase and mTOR-Dependent Regulation of Amino Acid Efflux from Lysosomes. *Science*, **2017**, *358* (6364), 807–813. https://doi.org/10.1126/science.aan6298.

[49] Tian, R.; Gachechiladze, M. A.; Ludwig, C. H.; Laurie, M. T.; Hong, J. Y.; Nathaniel, D.; Prabhu, A. V.; Fernandopulle, M. S.; Patel, R.; Abshari, M.; et al. CRISPR Interference-Based Platform for Multimodal Genetic Screens in Human iPSC-Derived Neurons. *Neuron*, **2019**, *104* (2), 239-255.e12. https://doi.org/10.1016/j.neuron.2019.07.014.

[50] Horlbeck, M. A.; Gilbert, L. A.; Villalta, J. E.; Adamson, B.; Pak, R. A.; Chen, Y.; Fields, A. P.; Park, C. Y.; Corn, J. E.; Kampmann, M.; et al. Compact and Highly Active Next-Generation Libraries for CRISPR-Mediated Gene Repression and Activation. *eLife*, **2016**, *5*. https://doi.org/10.7554/eLife.19760.

[51] Soyombo, A. A.; Tjon-Kon-Sang, S.; Rbaibi, Y.; Bashllari, E.; Bisceglia, J.; Muallem, S.; Kiselyov, K. TRP-ML1 Regulates Lysosomal pH and Acidic Lysosomal Lipid Hydrolytic Activity. *J. Biol. Chem.*, **2006**, *281* (11), 7294–7301. https://doi.org/10.1074/jbc.M508211200.

[52] Leray, X.; Hilton, J. K.; Nwangwu, K.; Becerril, A.; Mikusevic, V.; Fitzgerald, G.; Amin, A.; Weston, M. R.; Mindell, J. A. Tonic Inhibition of the Chloride/Proton Antiporter ClC-7 by PI(3,5)P2 Is Crucial for Lysosomal pH Maintenance. *eLife*, **2022**, *11*, e74136. https://doi.org/10.7554/eLife.74136.

[53] Bennett, N. K.; Nguyen, M. K.; Darch, M. A.; Nakaoka, H. J.; Cousineau, D.; Ten Hoeve, J.; Graeber, T. G.; Schuelke, M.; Maltepe, E.; Kampmann, M.; et al. Defining the ATPome

Reveals Cross-Optimization of Metabolic Pathways. *Nat. Commun.*, **2020**, *11* (1), 4319. https://doi.org/10.1038/s41467-020-18084-6.

[54] Samelson, A. J.; Ariqat, N.; McKetney, J.; Rohanitazangi, G.; Bravo, C. P.; Bose, R.; Travaglini, K. J.; Lam, V. L.; Goodness, D.; Dixon, G.; et al. CRISPR Screens in iPSC-Derived Neurons Reveal Principles of Tau Proteostasis. *bioRxiv*, **2024**, 2023.06.16.545386. https://doi.org/10.1101/2023.06.16.545386.

[55] C, P. B.; Am, G.; J, M.-P.; Z, Z.; Y, W.; Aj, S.; My, W.; A, E.; E, C.; L, F.; et al. Human iPSC 4R Tauopathy Model Uncovers Modifiers of Tau Propagation. *Cell*, **2024**, *187* (10). https://doi.org/10.1016/j.cell.2024.03.015.

[56] Cao, Y.; Li, R.; Shen, M.; Li, C.; Zou, Y.; Jiang, Q.; Liu, S.; Lu, C.; Li, H.; Liu, H.; et al. DDRGK1, a Crucial Player of Ufmylation System, Is Indispensable for Autophagic Degradation by Regulating Lysosomal Function. *Cell Death Dis.*, **2021**, *12* (5), 416. https://doi.org/10.1038/s41419-021-03694-9.

[57] Korolchuk, V. I.; Saiki, S.; Lichtenberg, M.; Siddiqi, F. H.; Roberts, E. A.; Imarisio, S.; Jahreiss, L.; Sarkar, S.; Futter, M.; Menzies, F. M.; et al. Lysosomal Positioning Coordinates Cellular Nutrient Responses. *Nat. Cell Biol.*, **2011**, *13* (4), 453–460. https://doi.org/10.1038/ncb2204.

[58] Amick, J.; Tharkeshwar, A. K.; Talaia, G.; Ferguson, S. M. PQLC2 Recruits the C9orf72 Complex to Lysosomes in Response to Cationic Amino Acid Starvation. *J. Cell Biol.*, **2020**, *219* (1), e201906076. https://doi.org/10.1083/jcb.201906076.

[59] Talaia, G.; Amick, J.; Ferguson, S. M. Receptor-like Role for PQLC2 Amino Acid Transporter in the Lysosomal Sensing of Cationic Amino Acids. *Proc. Natl. Acad. Sci. U. S. A.*, **2021**, *118* (8), e2014941118. https://doi.org/10.1073/pnas.2014941118.

[60] Ma, X.; Li, J.; Liu, N.; Banerjee, S.; Hu, X.; Wang, X.; Dong, J.; Liu, K.; Yang, C.; Dong, Z. Insights into the Distinct Membrane Targeting Mechanisms of WDR91 Family Proteins. *Structure*, **2024**, *32* (12), 2287-2300.e4. https://doi.org/10.1016/j.str.2024.09.023.

[61] Qian, Y.; Lee, I.; Lee, W.-S.; Qian, M.; Kudo, M.; Canfield, W. M.; Lobel, P.; Kornfeld, S. Functions of the α, β, and γ Subunits of UDP-GlcNAc:Lysosomal Enzyme N-Acetylglucosamine-1-Phosphotransferase *. *J. Biol. Chem.*, **2010**, *285* (5), 3360–3370. https://doi.org/10.1074/jbc.M109.068650.

[62] Hutagalung, A. H.; Novick, P. J. Role of Rab GTPases in Membrane Traffic and Cell Physiology. *Physiol. Rev.*, **2011**, *91* (1), 119–149. https://doi.org/10.1152/physrev.00059.2009.

[63] Liu, B.; Du, H.; Rutkowski, R.; Gartner, A.; Wang, X. LAAT-1 Is the Lysosomal Lysine/Arginine Transporter That Maintains Amino Acid Homeostasis. *Science*, **2012**, *337* (6092), 351–354. https://doi.org/10.1126/science.1220281.

[64] Zhu, H.; Li, Q.; Liao, T.; Yin, X.; Chen, Q.; Wang, Z.; Dai, M.; Yi, L.; Ge, S.; Miao, C.; et al. Metabolomic Profiling of Single Enlarged Lysosomes. *Nat. Methods*, **2021**, *18* (7), 788–798. https://doi.org/10.1038/s41592-021-01182-8.

[65] Kreitzer, F. R.; Salomonis, N.; Sheehan, A.; Huang, M.; Park, J. S.; Spindler, M. J.; Lizarraga, P.; Weiss, W. A.; So, P.-L.; Conklin, B. R. A Robust Method to Derive Functional Neural Crest Cells from Human Pluripotent Stem Cells. *Am. J. Stem Cells*, **2013**, *2* (2), 119–131.

[66] Pantazis, C. B.; Yang, A.; Lara, E.; McDonough, J. A.; Blauwendraat, C.; Peng, L.; Oguro, H.; Kanaujiya, J.; Zou, J.; Sebesta, D.; et al. A Reference Human Induced Pluripotent Stem

Cell Line for Large-Scale Collaborative Studies. *Cell Stem Cell*, **2022**, *29* (12), 1685-1702.e22. https://doi.org/10.1016/j.stem.2022.11.004.

[67] Christensen, K. A.; Myers, J. T.; Swanson, J. A. pH-Dependent Regulation of Lysosomal Calcium in Macrophages. *J. Cell Sci.*, **2002**, *115* (3), 599–607. https://doi.org/10.1242/jcs.115.3.599.

[68] Chakraborty, K.; Leung, K.; Krishnan, Y. High Lumenal Chloride in the Lysosome Is Critical for Lysosome Function. *eLife*, **2017**, *6*, e28862. https://doi.org/10.7554/eLife.28862.

[69] de Araujo, M. E. G.; Liebscher, G.; Hess, M. W.; Huber, L. A. Lysosomal Size Matters. *Traffic Cph. Den.*, **2020**, *21* (1), 60–75. https://doi.org/10.1111/tra.12714.

[70] Almeida, P. C.; Nantes, I. L.; Chagas, J. R.; Rizzi, C. C. A.; Faljoni-Alario, A.; Carmona, E.; Juliano, L.; Nader, H. B.; Tersariol, I. L. S. Cathepsin B Activity Regulation: HEPARIN-LIKE GLYCOSAMINOGLYCANS PROTECT HUMAN CATHEPSIN B FROM ALKALINE pH-INDUCED INACTIVATION*. *J. Biol. Chem.*, **2001**, *276* (2), 944–951. https://doi.org/10.1074/jbc.M003820200.

[71] Frost, L. S.; Dhingra, A.; Reyes-Reveles, J.; Boesze-Battaglia, K. The Use of DQ-BSA to Monitor the Turnover of Autophagy-Associated Cargo. *Methods Enzymol.*, **2017**, *587*, 43–54. https://doi.org/10.1016/bs.mie.2016.09.052.

[72] Millo, T.; Rivera, A.; Obolensky, A.; Marks-Ohana, D.; Xu, M.; Li, Y.; Wilhelm, E.; Gopalakrishnan, P.; Gross, M.; Rosin, B.; et al. Identification of Autosomal Recessive Novel Genes and Retinal Phenotypes in Members of the Solute Carrier (SLC) Superfamily. *Genet. Med.*, **2022**, *24* (7), 1523–1535. https://doi.org/10.1016/j.gim.2022.03.020.

[73] Lenk, G. M.; Park, Y. N.; Lemons, R.; Flynn, E.; Plank, M.; Frei, C. M.; Davis, M. J.; Gregorka, B.; Swanson, J. A.; Meisler, M. H.; et al. CRISPR Knockout Screen Implicates Three Genes in Lysosome Function. *Sci. Rep.*, **2019**, *9*, 9609. https://doi.org/10.1038/s41598-019-45939-w.

[74] Humphries, W. H.; Szymanski, C. J.; Payne, C. K. Endo-Lysosomal Vesicles Positive for Rab7 and LAMP1 Are Terminal Vesicles for the Transport of Dextran. *PLoS ONE*, **2011**, *6* (10), e26626. https://doi.org/10.1371/journal.pone.0026626.

[75] Olinger, E.; Wilson, I. J.; Orr, S.; Barroso-Gil, M.; Neatu, R.; Ambrose, J. C.; Arumugam, P.; Bevers, R.; Bleda, M.; Boardman-Pretty, F.; et al. Copy-Number Analysis from Genome Sequencing Data of 11,754 Rare-Disease Parent-Child Trios: A Model for Identifying Autosomal Recessive Human Gene Knockouts Including a Novel Gene for Autosomal Recessive Retinopathy. *Genet. Med. Open*, **2024**, *2*, 101834. https://doi.org/10.1016/j.gimo.2024.101834.

[76] Leray, X.; Conti, R.; Li, Y.; Debacker, C.; Castelli, F.; Fenaille, F.; Zdebik, A. A.; Pusch, M.; Gasnier, B. Arginine-Selective Modulation of the Lysosomal Transporter PQLC2 through a Gate-Tuning Mechanism. *Proc. Natl. Acad. Sci.*, **2021**, *118* (32), e2025315118. https://doi.org/10.1073/pnas.2025315118.

[77] Villa, S.; Jafri, Q.; Lazzari-Dean, J. R.; Sangha, M.; Olsson, N.; Lefebvre, A. E. Y. T.; Fitzgerald, M. E.; Jackson, K.; Chen, Z.; Feng, B. Y.; et al. BiDAC-Dependent Degradation of Plasma Membrane Proteins by the Endolysosomal System. *Nat. Commun.*, **2025**, *16* (1), 4345. https://doi.org/10.1038/s41467-025-59627-z.

[78] Tian, R.; Abarientos, A.; Hong, J.; Hashemi, S. H.; Yan, R.; Dräger, N.; Leng, K.; Nalls, M. A.; Singleton, A. B.; Xu, K.; et al. Genome-Wide CRISPRi/a Screens in Human Neurons

Link Lysosomal Failure to Ferroptosis. *Nat. Neurosci.*, **2021**, *24* (7), 1020–1034. https://doi.org/10.1038/s41593-021-00862-0.

[79] Fernandopulle, M. S.; Prestil, R.; Grunseich, C.; Wang, C.; Gan, L.; Ward, M. E. Transcription Factor-Mediated Differentiation of Human iPSCs into Neurons. *Curr. Protoc. Cell Biol.*, **2018**, *79* (1), e51. https://doi.org/10.1002/cpcb.51.

[80] Teter, O. M.; McQuade, A.; Hagan, V.; Liang, W.; Dräger, N. M.; Sattler, S. M.; Holmes, B. B.; Castillo, V. C.; Papakis, V.; Leng, K.; et al. CRISPRi-Based Screen of Autism Spectrum Disorder Risk Genes in Microglia Uncovers Roles of ADNP in Microglia Endocytosis and Synaptic Pruning. *Mol. Psychiatry*, **2025**, *30* (9), 4176–4193. https://doi.org/10.1038/s41380-025-02997-z.

[81] Bravo, A. M.; Typas, A.; Veening, J.-W. 2FAST2Q: A General-Purpose Sequence Search and Counting Program for FASTQ Files. *PeerJ*, **2022**, *10*, e14041. https://doi.org/10.7717/peerj.14041.

[82] Chen, E. Y.; Tan, C. M.; Kou, Y.; Duan, Q.; Wang, Z.; Meirelles, G. V.; Clark, N. R.; Ma'ayan, A. Enrichr: Interactive and Collaborative HTML5 Gene List Enrichment Analysis Tool. *BMC Bioinformatics*, **2013**, *14*, 128. https://doi.org/10.1186/1471-2105-14-128.

[83] Kuleshov, M. V.; Jones, M. R.; Rouillard, A. D.; Fernandez, N. F.; Duan, Q.; Wang, Z.; Koplev, S.; Jenkins, S. L.; Jagodnik, K. M.; Lachmann, A.; et al. Enrichr: A Comprehensive Gene Set Enrichment Analysis Web Server 2016 Update. *Nucleic Acids Res.*, **2016**, *44* (W1), W90-97. https://doi.org/10.1093/nar/gkw377.

[84] Xie, Z.; Bailey, A.; Kuleshov, M. V.; Clarke, D. J. B.; Evangelista, J. E.; Jenkins, S. L.; Lachmann, A.; Wojciechowicz, M. L.; Kropiwnicki, E.; Jagodnik, K. M.; et al. Gene Set

Knowledge Discovery with Enrichr. *Curr. Protoc.*, **2021**, *1* (3), e90. https://doi.org/10.1002/cpz1.90.

[85] Concordet, J.-P.; Haeussler, M. CRISPOR: Intuitive Guide Selection for CRISPR/Cas9 Genome Editing Experiments and Screens. *Nucleic Acids Res.*, **2018**, *46* (W1), W242–W245. https://doi.org/10.1093/nar/gky354.

[86] Ran, F. A.; Hsu, P. D.; Wright, J.; Agarwala, V.; Scott, D. A.; Zhang, F. Genome Engineering Using the CRISPR-Cas9 System. *Nat. Protoc.*, **2013**, *8* (11), 2281–2308. https://doi.org/10.1038/nprot.2013.143.

[87] Stirling, D. R.; Swain-Bowden, M. J.; Lucas, A. M.; Carpenter, A. E.; Cimini, B. A.; Goodman, A. CellProfiler 4: Improvements in Speed, Utility and Usability. *BMC Bioinformatics*, **2021**, *22* (1), 433. https://doi.org/10.1186/s12859-021-04344-9.

[88] Alquezar, C.; Schoch, K. M.; Geier, E. G.; Ramos, E. M.; Scrivo, A.; Li, K. H.; Argouarch, A. R.; Mlynarski, E. E.; Dombroski, B.; DeTure, M.; et al. TSC1 Loss Increases Risk for Tauopathy by Inducing Tau Acetylation and Preventing Tau Clearance via Chaperone-Mediated Autophagy. *Sci. Adv.*, **2021**, *7* (45), eabg3897. https://doi.org/10.1126/sciadv.abg3897.

[89] Yates, D. A Neuronal Subcompartment View of ATP Production. *Nat. Rev. Neurosci.*, **2024**, *25* (3), 142–142. https://doi.org/10.1038/s41583-023-00792-9.

[90] Area-Gomez, E.; Guardia-Laguarta, C.; Schon, E. A.; Przedborski, S. Mitochondria, OxPhos, and Neurodegeneration: Cells Are Not Just Running out of Gas. *J. Clin. Invest.*, **2019**, *129* (1), 34–45. https://doi.org/10.1172/JCI120848.

Publishing Agreement

It is the policy of the University to encourage open access and broad distribution of all theses, dissertations, and manuscripts. The Graduate Division will facilitate the distribution of UCSF theses, dissertations, and manuscripts to the UCSF Library for open access and distribution. UCSF will make such theses, dissertations, and manuscripts accessible to the public and will take reasonable steps to preserve these works in perpetuity.

I hereby grant the non-exclusive, perpetual right to The Regents of the University of California to reproduce, publicly display, distribute, preserve, and publish copies of my thesis, dissertation, or manuscript in any form or media, now existing or later derived, including access online for teaching, research, and public service purposes.

DocuSigned by:
Mackenzie Welch
DD9262D9CCF7454...
Author Signature

8/29/2025
Date